Improving the Wear Resistance of Barite Mining Tools

By

EBECHIDI NNAEMEKA SAMSON

A THESIS SUBMITTED TO THE AFRICAN UNIVERSITY OF SCIENCE

AND TECHNOLOGY, ABUJA – NIGERIA

IN PARTIAL FULFILLMENT OF THE REQUIREMENTS FOR THE AWARD OF

MASTER OF SCIENCE

IN MATERIALS SCIENCE AND ENGINEERING

SUPERVISOR: **PROF W. O. SOBOYEJO**

DECEMBER, 2014

Improving the Wear Resistance of Barite Mining Tools

A THESIS APPROVED BY THE MATERIALS SCIENCE AND ENGINEERING DEPARTMENT

BY

RECOMMENDED: _____

SUPERVISOR, PROF. WOLE SOBOYEJO

APPROVED: _____

HEAD, DEPARTMENT OF MATERIALS SCIENCE AND ENGINEERING

_____

CHIEF ACADEMIC OFFICER

_____

DATE

Dedication

I dedicate this thesis to God Almighty, Prof W. O. Soboyejo for inspiring my life and to my mum Mrs Ngozi Ebechidi for her incredible support.

Acknowledgement

Special thanks go to God for the gift of life and the privilege to have completed this MSc program. I thank Prof W. O. Soboyejo, my supervisor, for giving my life a true meaning. Thanks to my sponsor, African Development Bank (AfDB) for giving me the scholarship to embark on this program, here at AUST. Dr. O. Shola, Dr. A. O. Omololu, Dr. A. R. Adetunji, Dr. Z. Kana and Dr. Adesina (NTNU) were tremendous in supporting me in various ways as lecturers and advisers.

I thank very heartily Engr. D. Y. Yusuf of SCC Pipe Yard, Bwari – Nigeria. Without him and his team at the lab, this work would not have succeeded the way it did. Engr. Dr. Bamali and Mr. Romanus were very helpful with getting me barites from Cross-River State. Miss Theresa Ezenwafor and Engr. Ogunkoya of Engineering Materials Research Institute (EMDI) – Akure, Nigeria helped with the XRD results of the barite.

I specially recognize the following PhD candidates here at AUST for their amazing and selfless support in making this work successful: Emmanuel K. Arthur, Edward K. Ampaw, Vitalis Anye, Kehinde Oyewole and Joseph Asari. Paul Dickson, my colleague in Petroleum Stream, Mr. O. D. Edugbeke of Nigerian Geological Survey Agency, Mr. Iyke Ogbu of Mobil Plc, and Engr. Oluchi Nwoko of Seventy One Nigeria Ltd helped my understanding of barite mining and its application in the oil and gas industry.

I want to thank my fellow MSc. Candidates. My mum showed me incredible support. I thank my siblings: Onyeka, Simeon and Joy. Finally, I thank my endless list of friends Jude Oketta, John Olatunde, O. Nwajagu, Genesis Agbo, E. Okpara, Ann Okagbue etc.

Abstract

Wearing of mining tools leads to high replacement costs, machine downtime and loss of business opportunities. This work was however, aimed at improving the wear resistance of AISI 1065 and 1070 proeutectoid steels used for (barite) mining operations. To achieve this, the case hardening method adopted was pack-cyaniding with dried and pulverized cassava leaves (a type of carbonitiriding) at 700, 800, 850 and 900°C. After the carbonitriding process, the 1065 steel was quenched and tempered at 300°C for 3hrs, whereas the 1070 was air cooled. As a result, the tempered martensitic 1065 steel formed, showed an increase in hardness of 706 HV over that of 540 HV obtained previously in literature with the same method. Pin-on-disk wear experiments were conducted on the as-received and carbonitrided pin samples. The result showed that at 900°C, the lowest wear rate, lowest coefficient of friction, highest hardness and highest strength were observed for the 1065 carbonitrided steel. Charpy impact results indicated that the toughness of the carbonitrided samples decreased, and reasons for this decrease were explained. The implication of these results revealed that hardening of steels with locally pulverized cassava leaves is cost effective and environmentally safer than conventional means.

Keywords: barite, mining, pack-cyaniding, carbonitiriding, wear resistance.

Table of Contents

List of Figures

List of Tables

1.0 Introduction

1.1. Background and Introduction

Barite, consisting of barium sulphate ($BaSO_4$), is a non-metallic mineral, chemically stable, with Moh's hardness of 3-3.5 and a density of 4.48 g/cm^3. Some 77% of barite worldwide is used as a weighting agent for drilling fluids. It is used in oil and gas exploration to suppress high formation pressures and prevent blowouts. As a well is drilled, the bit passes through various formations, each with different characteristics. The deeper the hole, the more barite is needed as a percentage of the total mud mix[1].

Nigeria holds the fourth largest deposit of barite in the world. Ironically, Nigeria is not anywhere in the list of the 16th largest producers of barite in the world. According to records, China the largest producers, produces 3.6 Million MT per annum; India, 1Million MT per year and USA, 675 Thousand MT per year. Within Africa, Morocco is the 5th largest in the world followed by Algeria the 14th with production capacities of 142 Thousand MT and 47 Thousand MT per annum respectively. Nigeria is among the others. The others does not account up to 5% of world population. Principal factors responsible for this are the importation of barite and lack of LPOs from oil and gas companies to local producers. As a result, local investors are not motivated to consider this as a viable option, whereas, local miners cannot meet up with the demand.

The two main areas of concern are the mining and the processing. About 80% of the mining activities are locally done, with diggers, hoes and shovels. This is predominantly the case in Nasarawa, Benue and Cross Rivers States where high level of barite mining occurs. Even the Asians involved in this production still employ local miners for their mining operations.

The output of the use of pickaxes, shovels and hoes are grossly limiting. Scientists and engineers did estimate that the mining tools (pickaxes and shovels) used as early as 5000 B.C. for mining copper at the surface of Michigan Upper Peninsula would take 10,000 people roughly 1,000 years to excavate the 1.5 billion pounds of copper from that area[2]. In contrast, it would take approximately 38.5 hours for the fabled Big Muskie dragline to excavate the same amount of material[3]. Notwithstanding, the challenge of both sub-optimal and optimal mining tools still persists.

The oscillating loads associated with mining and processing tools can result in the wear and fatigue of drill bits, mining tools and processing equipment. The high cost of mechanized mining and processing equipment impacts negatively on investment interests. Currently, there are no large scale barite processing facilities in the country. The ones present do not process to API standard that requires at least 97% of the material, by weight, to pass a 200-mesh (75-μm) screen. Consequently, much of the barites used in Nigeria's oil and gas industry are imported even though Nigeria holds about the fourth largest deposits of barite in the world, with presence in 9 states of the federation.

The demand for this very important mineral is quite high. In Nigeria, estimated demand is up to N255,000.00 MT per annum. The local market price of this mineral is about N50,000.00 per ton, but it is imported at N170,000.00 per ton. Local involvement is poor in terms of quality and quantity of output and industrial participation is nearly zero.

1.1.1. Problem Statement

Barite occurs in limestone and sandstones. The hardness of barite mineral in relation to impurity minerals present in a deposit principally imposes significant damage to mining tools. The hardness of barite is about 1.7 to 2.0GPa. That for quartz and silica, accounting up to 60% of the earth crust, ranges from 7.5 to 12GPa[4]. In a barite vein, some report has it that about 6 – 8% of silica is present. This is in exception of the surface or underground material to be excavated before reaching the vein. With the presence of these hard minerals, mining tools – including hard martensitic steels with hardness range of 7 – 8GPa still wear away over time[4].

In mining, efficient and very functional mining tools are critical for success. Failure due to wear reduces the lifespan of these tools and thus increases mining cost. The main wear mechanism present in these tools is the relative wear due to metal-mineral contacts involving impact and sliding. For parts subjected to wear and impact, the main steel selection criteria are usually based on the surface hardness and bulk toughness of the component. Asides this, corrosion resistance is another

important selection factor[5] as these tools sometimes operate in wet conditions. Since steels of these type are ductile metals, fatigue and fracture toughness may not be of critical concern. This can be an exception when the preparation methods introduce defects that are failure zones in the bulk steel.

The high cost of replacing worn parts is alarming and has grave economic consequences. When the parts are replaced, the machine is laid to rest, leading to production losses and in some cases loss of business opportunities. While this is a problem, seeking for ways to reduce wearing is the basic focus of this thesis work. Hence, surface hardening of steels is the option that was considered.

1.2. Unresolved Issues

Although enormous research has been done in this area, wearing of mining tools still persists. When the surface of the tools become hardened, other property of the steel gets hampered, but a lot of these researches were made without a holistic consideration of the balance of material property for effective application.

In hardening of steels, the gases, liquids or solids used for this process are usually expensive and sometimes not readily available. When used, they are not environmentally friendly due to their high toxicity. They pollute the environment and affect humans negatively.

1.2.1. Aims and Objectives

The goal of this research work is to resolve the issues enumerated above as much as possible using scientific methods within reach. To this, effort is being made to

1. Improve the wear resistance of steels by increasing the hardness and strength of steels through the diffusion of carbon and nitrogen into interstitial holes in the metal. Then, carry out other heat treatment processes to achieve and validate a balance of material property for this application.
2. It is equally intended that the hardness and strength of the steel is increased through waste to wealth scheme. This is by using locally available cassava leaves that are air dried, pulverized and mixed with an energizer to activate the diffusion of carbon and nitrogen into the metal.

1.3. Scope of Work

Wear resistance of materials are determined by conducting wear tests. One of such tests is the pin-on-disk testing using a laboratory equipment called the tribometer. The ASTM G99-95 standard describes a standard process of using this equipment to simulate the wear behavior of metals[5]. In this equipment, the test was carried out at selected parameters that held constant while varying the others. The constant parameters include normal load on pin, sliding velocity and controlled conditions of temperature and relative humidity[6]. However, the total sliding distances varied, upon which measurements were made. Prior to this process, the steels were

carbonitrided at varying temperatures and effort was made at interpreting the wear mechanism responsible for the wearing of steels.

So, as a way of summary, however:

- Chapter 2 focused on brief introduction to the state of barite mining in Nigeria as well as the estimated reserve of barites in Benue, Taraba, Zamfara, Nasarawa and Cross River State. Extensive attention was given to wear researches in this area to form a framework for this work.
- Chapter 3 simply discussed the methodologies employed in carbonitriding and conducting wear experiments.
- Chapter 4 gave the summarized results of the entire work as well as discussion on the said results.
- In Chapter 5, the work was concluded, recommendations were made and brief details of future work were highlighted, with sufficient data for further analyses.

2.0 Literature Review

2.1. Introduction

Nigeria has an extensive, but sporadic history of mining. In the past, tin, columbite and coal were the prominent minerals mined and exported[7]. The Ministry of Mines and Steel Development (MMSD) promotes private sector participation in the development of the mining sector. This is brought about by the initiation of new policies and frameworks that aims at achieving the following:

1. Increase in GDP contribution by the minerals sector,
2. Generation of quality geo-mapping and geoscience data,
3. Formalizing Artisanal and Small Scale Mining (ASM) operators,
4. Attaining high poverty reduction through ASM operation,
5. Generation of employment opportunity,
6. Wealth creation through value addition,
7. Increase in capacity of mineral based industries, and
8. Attraction of foreign direct funding and private investment capital[7].

The result of this framework will foster growth at both high and low levels of the chain.

2.2. Barite Exploration in Nigeria

2.2.1 Occurrences

Several minerals exist in the country. One of interest is barite. It has its application in various fields but particularly in the oil and gas industry.

Associated with the lead-zinc deposits, barite occurs in Nigeria as vein infilling materials. It occurs in both Pre-Cambrian basement and Cretaceous sedimentary rocks of the lower and middle Benue valley. The vein width ranges from a few centimeters to 5.3 meters. Whereas, the length spans from few meters to greater than 4.5km. In Nigeria, barite commonly occurs as white, reddish brown and clear varieties with specific gravity varying between 3.5 and 4.4[7].

In 1959, a reserve of 41,000 tons for the Benue valley deposits was estimated in a preliminary survey by the Geological Survey of Nigeria. In addition, 70,000 tons of barite in Azara deposit in Nasarawa State was surveyed by the Nigerian Mining Corporation. Recently, the reports from the Nigerian Geological Survey Agency evaluated the combined deposits in four states of the federation to stand at 21,123,913 metric tons. These states include Benue, Cross River, Nasarawa and Taraba States[7].

2.2.2 Barite in Benue State, Nigeria

In Benue State – Nigeria, barite deposit is housed in both the Pre-Cambrian igneous-metamorphic rocks and the Benue trough sedimentary sandstones and shale

formations. The mineralization of barite deposits is in the form of hydrothermal solutions filling fissures with barites, formed by the closing in of the Benue trough during the Santoninan[7].

Occurring as white, reddish brown and clear varieties, barites in Benue State has specific gravity (SG) ranging from 3.7 to 4.4. Chemical analysis conducted in most samples showed the presence of 76 – 87% $BaSO_4$, 5 – 21% Silica and up to 3% Iron oxide[7].

Barite veins in this area are commonly 3m wide and 20m deep. However, when exposed, they do not persist over long distances. The average SG of 4.0 and the estimated reserve of 307,657 metric tons makes barite mining viable in this state[7].

2.2.3 Barite in Taraba State, Nigeria

Taraba State, Nigeria hosts barite in five of its LGAs, namely: Sardauna, Karim Lamido, Yoro, Lau and Ibi. The deposits are in porphyritic granites and fine grained sandstones. Vein width ranges from 3.5 to 5 meters, whereas its length persists over 3,500 to 5,000m range. To obtain grade barite for industrial applications, the barites in Taraba State consists of Quartz and sulphide minerals like galena[7].

The inferred barite resource in Taraba State, Nigeria is 8,960,000 metric tons, measured to 20m depth. The quality of deposit is very good; with most of the resource having SG close to 4.2. Considering the size of individual veins present,

investment in heavy equipment to mine at greater depth is considered worthwhile[7].

2.2.4 Barite in Zamfara State, Nigeria

In Zamfara State – Nigeria, barite mineralization is linked to epigenetic hydrothermal fluids, which leached barium from adjacent rocks and precipitated the barites in the veins. This extensive deposit depicts wide variations in certain properties, more especially its thickness. The vein lengths are greater than 100m, whereas its widths vary from a few centimeters up to several meters (0.6m – 2m range)[7].

Barites in Zamfara State, Nigeria occur in the following locations, namely:

1. Dareta near Anka, Anka Local Government.
2. Rekebu near Chafe, Chafe (Tsafe) Local Government.
3. Yarkatsina (Gidan Saro) Bungudu Local Government, and
4. Tofa forest reserve, Gusau Local Government.

With uneven fractures, the barites in these locations are massive to granular; having varying colors from white to reddish brown[7].

2.2.5 Barite in Nasarawa State, Nigeria

Assorted sedimentary rocks (shale, mudstones, siltstones and limestone etc.) host barite in Nasarawa state, Nigeria. The occurrence varies in width between a few centimeters to 3.5m and in length between just under 1,000 to over 4,000m. The specific gravity (SG) of Nasarawa state barites are between 3.9 and 4.4. This grade

range is within the 4.2 minimum specification of the American Petroleum Institute (API)[7].

However, some tested samples with 3.6 SG are equally present. These are the ones that are rich in silica, and are not suitable except they are beneficiated. Other impurities present include quartz, celestite ($SrSO_4$) and iron oxide[7].

The estimated amount of barite resource in Nasarawa is put at 3,243,376 metric tons, calculated at an average SG of 4.0 and a projected vein depth of 20m[7].

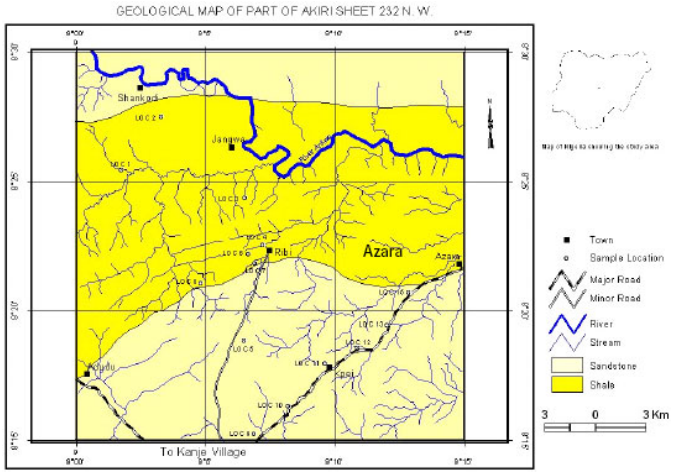

Figure 2-1: Geological map of part of Akiri sheet 232 N.W., Azara-Nasarawa State, Nigeria.[8]

2.2.6 Barite in Cross River State, Nigeria

Hosted in both hard and soft rocks, the barite veins in Cross River State, Nigeria are in 35 mineralized locations with 11 in sedimentary areas. This study by the Nigerian Geological Survey Agency showed that the mineralized areas are divided into two; namely the south consisting of Biase and Yakkur LGA and the north comprising of

Obubra, Ikom and Yala LGA. In the north, sedimentary rocks host more of the barites than in the south. Only 2 out of 18 locations in the south are in sedimentary rocks[7].

The width of the veins is often between 2.5 and 5.3m, while the length ranges from 1,000 to 6,000m. With varying SG of 3.5 to 4.4, the estimated reserve in the entire state is 8,612,880 metric tons, distributed almost evenly between the north and the south. This estimate is most likely to increase as new veins are discovered in the future. However, resource extraction in the northern zones is easier than those in the south as a result of the presence soft host rock in majority[7]. Notwithstanding, mining in the state is viable, especially with its proximity to the oil and gas industries than other locations in the country.

2.3 Barite Characterization

2.3.1 Chemical Composition

To design and fabricate an optimal processing plant, the chemical compositions of the various deposits are to be characterized. This would provide the basis for what equipment is needed in the beneficiation train assembly, especially that barite deposits and their constituent impurities in Nigeria varies from one place to another. For example, the chemical analysis of the barite in Azare of Bauchi State is shown in the table below. Details of the characterization and the comparisons with that of refined barite in Turkey are also shown.

Table 2-1: Chemical Analysis of Azare Barite in Bauchi State, Nigeria with that in Turkey[9]

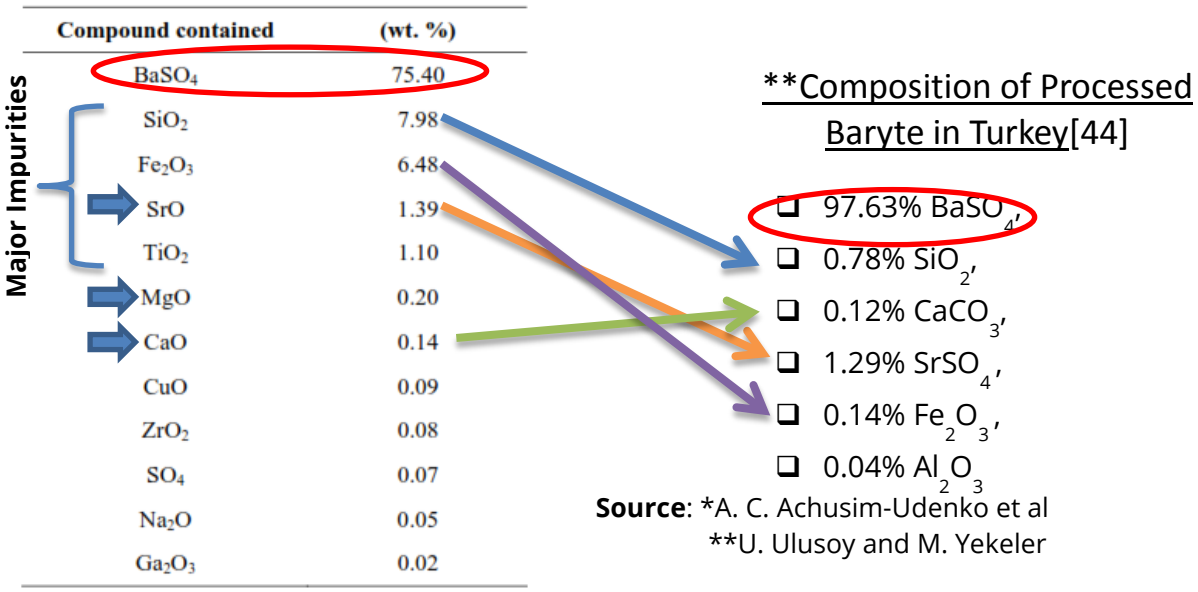

From the table above, it can be seen that the goal is to take the grade of ore in the left to that on the processed barite in the right. To do this, the impurities are to be removed or grossly minimized and that is where the cost of processing comes in. To remove the denoted major impurities, gravity separation can be used for the SiO_2, whereas a magnetic separator is to be used to remove the Fe_2O_3. This is because, the specific gravity of SiO_2 to that of $BaSO_4$ is wide and obeys the concentration criterion (further details on this is covered under the section on barite beneficiation). Also, since $BaSO_4$ is non-magnetic, it can be separated from the more magnetic Fe_2O_3. Other processing methods can be adopted to remove other impurities. These methods include flotation, leaching etc.

2.4 Barite Mining

2.4.1 Brief History of Mining in Nigeria

Organized mining in Nigeria started around 1939 through private owned foreign companies. The first legislation on mining was enacted in 1946 and was only reviewed in 1999. Both laws (1946 and 1999) have no provision for artesanal mining. The collapse of big mining companies in the early 70s led to massive unemployment of mine workers without any means of livelihood. Many of them went into illegal mining activities to survive.[8]

Increased global demand for solid minerals and the introduction of SAP (Structural Adjustment Programme) created ready export markets for products of illegal mining activities; this also led to the emergence of middlemen and mineral smugglers. The official response to these phenomena was wild and not sustained. Illegal mining activities have continued to flourish uncensored, due also to lack of alternative gainful employment. Government can no longer ignore these illegal activities because of the huge revenue loss and the attendant environmental degradation as well as other social problems.[8]

2.4.2 Sub-optimal Mining Operations

It is very obvious artisanal mining characterizes barite mining in Nigeria. This activity turned into a lucrative business immediately after the abandonment of the mechanized method of mining in the 80s. Ever since then, the exploration of barite in

Nigeria has been manually characterized by the use of primitive tools such as diggers and shovels usually on a small scale. Under this condition, certainly only the surface or near surface veins are exploited. Also, the conditions under which the local miners work, is highly risky and could result in loss of lives and property. The exploitation is done indiscriminately either by individuals or groups. However, there appears to be some coordination in the manner in which each individual or groups go about the exploitation. The environmental impact is great. Apart from the devastation of arable farmland, very large and deep pits are left behind after exploitation which could form death traps[8].

Figure 2-2: Barite mines showing different vein orientations at the Wuse mine site near Azara, Nasarawa, Nigeria[8].

2.4.3 Advanced Mining and Crushing Operations

Barite deposits can be divided into the layered type deposit, vein type deposit, transformed vein type deposit and accumulation type deposits. Commercial barite mining includes open-pit mining and underground mining with the former being the most popular method. In open-pit mining, barites are usually quarried at residual talus deposits and outcrops and shallow depth ore deposits. In underground mining, barites are usually quarried through the shrinkage method, filling method and stage caving method. The mining equipment used in underground mining consists of ore trucks, inclined shaft hoist, local exhaust ventilation fan and underground support. Machines used in open-pit mining include power shovels, draglines, loaders and dump trucks to haul to crushing sites. The broken ore is trucked to the processing plant where it may be washed by log washer or trommel screen to remove adhering clay and low-grade fines before reduction by jaw or impact crusher to 25 cm or finer for further processing. The degree of further processing and concentration depends on the grade of ore, identified end use, and liberation size (i.e. the size at which the barite is essentially free of contaminating impurities). If a further size reduction is required, this can be accomplished by jaw crusher, impact crusher, cone crusher, or roll crushers[10]**.**

2.5 Surface Hardening and Surface Modification of Metals

There are various surface hardening and surface modification techniques that are used in the steel industry. The first set of surface-hardening techniques is mostly appropriate for producing steels with hard-wearing surface layers and tough inner cores. These include, gas carburizing, carbonitriding, nitriding and induction surface heating. The second set of these techniques is those that are localized. They include flame hardening and laser hardening. Other kinds of surface treatment processes include plasma carburizing, plasma nitriding and plasma spray coatings (for the oxidation protection of nickel-base superalloys for gas turbines)[11].

However, for the modification of metals to improve their hardness and wear properties, the following techniques are adopted: ion implantation and physical vapour deposition[11]. Of these techniques, carburizing and nitriding would be discussed. However, more attention would be paid to carbonitriding and boronitriding as they are the two surface hardening techniques used in this research work.

2.5.1 Carburizing of Steels

Steels containing 0.1 to 0.2 wt% carbon are typical for the carburization process. In this process, carbon is introduced into the surface layers (or case) of these low carbon steels, to raise the carbon content to about 0.8 to 1.0 wt% C. This practise is carried out to diffuse carbon into the surface of the steel substrate at elevated temperatures[12]–[16]. Carbon and alloy content, machinability, grain growth

characteristics and cost are some of the many variables that determine the selection of steel for carburizing[11].

For FCC-austenitic steels, the carbon is introduced at temperatures above the upper transformation temperature (Ac1). This is the austenitic region where appreciable interstitial solid solubility of carbon is possible. In Fe-C alloys, the carbon in iron ranges from about 0.8% at 723℃ to about 2.0% at 1148℃. However, about 0.02% maximum solubility of carbon in iron is observed in BCC ferrite below 723℃. This low solubility makes carburization not possible in this instance[11].

Although carburizing can be done on low and high temperatures like 790℃ (1400℉) and 1095℃ (2000℉) respectively, they most frequently are performed between 850 to 950℃ (1550 - 1750℉) range. The limitation of furnaces is principal to the high-temperature limits. However, during the long high temperature carburizing treatments, carburized steels should be deoxidized (aluminium-killed) to prevent austenitic grain coarsening[11].

After carburizing, a martensitic structure is usually produced at the surface layer by quenching. The carburizing treatment produces steel with a hardened surface and a core with low strength, high ductility and toughness, which is characteristic of a low-carbon steel. Ferrite-pearlite microstructures with relatively low strengths are usually formed in the cores of plain-carbon steels. However, low-alloy steels form martensitic cores with improved strength and toughness. Due to their quench rates, they have less tendencies to distortion and crack during quenching[11].

In the industry, carburizing is widely used for machine components and heavy-duty gears where surface resistance to wear, fracture toughness and contact/bending fatigue is required[11]. For mining tools, carburizing will increase their resistance to wear, fatigue and fracture.

Selcuk et. al. in 2003 studied the increase of hardness of both 1020 and 5115 steels after being carburized at 930°C. The carburization of both steels was done in a liquid media for 1.5, 3 and 4 hrs. After which, the samples were quenched in an oil medium at 50°C for 30mins, and then tempered at 200°C for 1 hr. The result of the increase gave values as high as 616 HV for 1020 steel and 795 HV with core hardness of 375 HV for 5115 steel[17].

Pressurized carburization is more recent whereby initial pressure is applied on the sample to increase the interaction between the powder and the surface of the substrate. The pressure plastically deforms the surface asperities of the steel during this process such that the application of external force fosters diffusion of carbon into the surface of the steel. In a work carried out by Abdul Azis et. al. in 2012, DSS stainless steel was carburized at 950°C for 4 hrs under 74 MPa pressure. After air cooling to room temperature, the hardness increased from 340 HV to 1512 HV at carburized layer range of 25 - 64μm[16].

2.5.2 Nitriding of Steels

In nitriding of steels, nitrogen in the atomic form is introduced into the surfaces of certain grades of steels, under the ferritic (BCC) condition. During this process,

nitrides form at or near the surface of steels containing alloying elements like molybdenum, chromium, vanadium and aluminium. These nitrides provide the hardening effect at treatment temperature ranging from 495 to 595℃ (925 – 1100℉) for 1 to 100hrs depending on the steel type and treatment depth[11].

Nitriding does not require heating the steel to austenitic temperatures nor subsequent quenching into martensitic structures. It is rather done in lower temperatures than carburizing, thereby producing workpieces with less distortion and deformation. Volume changes are negligible as no austenitic-ferritic transformation occurs during the process[11].

Ammonia gas is typically used as it dissociates on a steel surface in line with the following reaction:

$$NH_3 \leftrightarrow N + 3H$$

Surface nitriding of steels give rise to the following advantages:

1. Provision of high surface hardness
2. Increase of wear resistance and antigalling properties
3. Increase of fatigue life and
4. Provision of a heat-resistant surface (up to the nitriding temperature).

Nitrided surfaces are harder than carburized ones. They are quite stable up to the nitriding temperature. They have excellent resistance against heat generated friction in parts[11]. The wearing of tool surfaces can, amongst other things, be attributed to the temperature at impact points between the tool and the contact surface. Hence, nitriding is one way to reduce wear as a result of temperature gradient.

2.5.3 Carbonitring of Steels

Carbonitriding is not a type of nitriding, but a modified type of carburizing. The addition of ammonia to the carburizing gas at lower temperatures, at less cost and for shorter times are all there is to the modification. During the process, nitrogen diffuses in the steel surface layers along with carbon resulting to a hard, wear-resistant layer in steels[11].

Carbonitrided surface has higher hardenability than carburized surface of the same steel. The presence of nitrogen increases hardness, reduces distortion and retains or stabilizes the austenite phase, especially in alloy steels. Carbonitrided surface has higher resistance to softening during tempering but regrettably, lower case depth than carburized surface (i.e. from 0.075 to 0.75 mm [0.003 – 0.030 in] thick)[11].

The 1000, 1100, 1300, 4000, 4100, 4600, 5100, 6100, 8600, and 8700 steel series with about 0.25% carbon contents are good candidates for carbonitriding. For many steels with 0.35 to 0.50% C range, carbonitriding can sometimes be done up to shallow depths of 0.3mm (0.01in). This produces hard-wearing surfaces with tougher through-hardened cores[11].

Again, Selcuk et. al., 2003 studied the effect of carbonitriding on 1020 and 5115 steel. The hardness produced after this process was 743 HV for the 1020 steel and 820 HV with core hardness of 460 HV for the 5115 steel. This experiment was done with 12 m^3/h endogas plus 0.8 m^3/h ammonia gas at 860°C for 3.5 hrs. and were quenched in oil at 50°C for 30min, and then tempered at 200°C for 1 hr. The various hardness of

the carburized layer is shown by the plot in Fig 2.3[17]. These results, though impressive, do have implications on the cost of the gas and its environmental impact.

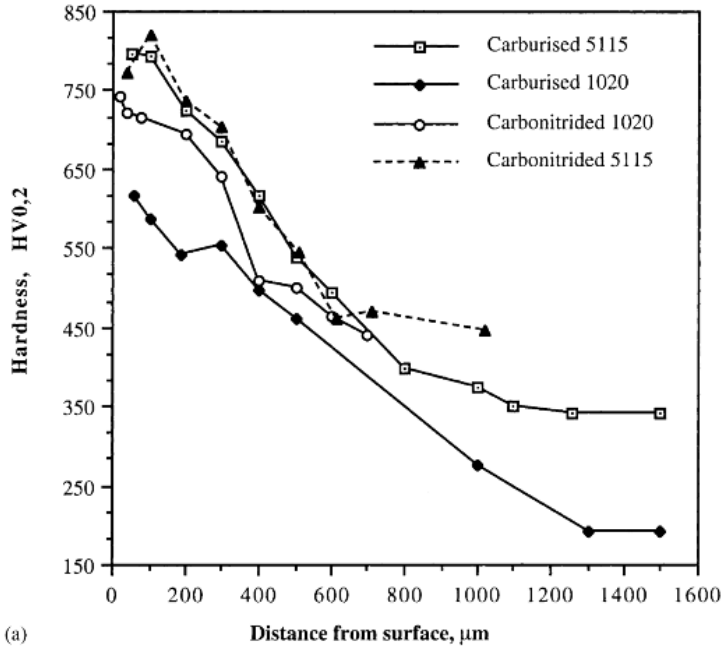

Figure 2-3: Hardness distribution of the test materials carburized (930°C, 3hrs) and carbonitrided (860°C, 3.5hrs)[17].

Ibironke et. al. in 2004 led a pioneer work in pack cyaniding of made in Nigeria low carbon steels. The samples were subjected to pack-carburizing medium using dry and pulverized cassava leaves. The intention was to harness the carbon and nitrogen content in the leaves for strengthening and hardening the surface of steels. This was a novel work as it was to replace conventional mode of using potassium ferrocyaniding, which is toxic in nature[18].

Studies have shown that the cyanide content in cassava leaves is between 3 – 4%, which is 100 times that in cassava tubers[18], [19]. The cyanided case of the steel is well known to contain C and N, with hardness reaching 800 – 900 HV. Having

structure similar to that of carburized layer, it contains a thin high N with ϵ-phase. When hardened by quenching, the martensitic steel that is formed has both C and N being dissolved accordingly. The hardness, wear resistance, fatigue limit and corrosion resistance is improved dramatically[18], [20].

Ibironke et. al, 2004 realized that the highest hardness value achieved in pack-cyaniding for 2, 3 and 4 hrs diffusion times were at 483.3, 519.1 and 540.02 HV respectively. In like manner, the highest case depths of 0.65, 1.05 and 1.65mm were obtained for the 3 different diffusion times mentioned above. After modeling for 5 and 6 hours, the resultant case depths increased to 1.68 and 1.90 mm respectively[18]. The plot of hardness to case depth is shown below.

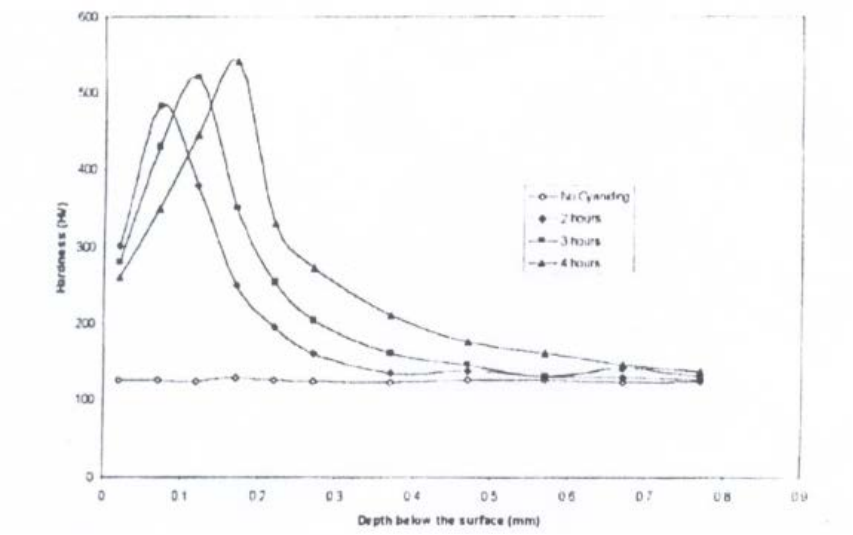

Figure 2-4: Plot of hardness against depth below the surface for the experimental data[18].

2.5.4 Boronizing of Steels

Boronizing is one of the most widely used method of hardening the surface of metals against abrasive, adhesive and sliding wear and frictional contacts[21][22]. In the past 40 years, it has exhibited excellent wear resistance for many tribological applications[22]–[24]. The hardness comes from formation of borides at the surface after the diffusion of boron atoms into the metal[21], [22], [25]. This is possible because the boron atoms are small in size and has the capability of forming many compounds with metals[26], [27], [22]. Boronizing ferrous metals are usually done between 840 - 1050°C. These can be done in gaseous, liquid or in solid form[21], [22], [28]. Pack boronizing usually comprise 5%B_4C as the source, 5% KBF_4 as the activator and 90% SiC as the diluting agent[28], [29]. The samples are normally placed in a container filled with the powder, then heated to the desired temperature and prescribed time, prior to being cooled[28]. The result for the work done by Tabur et. al. in 2009 showed increase of hardness from 220 HV to 1650 HV and 1850 HV at 850°C for 2hrs and 950°C for 6hrs respectively[22]. The result for the work done by Meric et. al., 2005 showed an extensive increase in hardness of ductile iron from 347 to 2685 HV, for grey iron 306 to 2465 HV and for compacted graphite iron 289 to 2685 HV[30].

2.6 Diffusion Kinetics

The migration of carbon and nitrogen atoms into the surface of steels is by diffusion process. Recall that the rate of diffusion depends on the concentration gradient and diffusion coefficient according to the relation:

$$J = -D\frac{\partial c}{\partial x} - - - - - - - - 2.1$$

Where J is diffusion flux (kg/m^2.s or atoms/m^2.s) representing the quantity of diffusing substance through a unit area perpendicular to the plane. D is diffusion coefficient (m^2/s), and $\partial c/\partial x$ is concentration gradient (kg/m^3 or g/cm^3)[18], [31].

Recall also that diffusion coefficient is a function of temperature, T (K). The following equation depicts such relation:

$$D = D_o \exp\left(\frac{-Q}{RT}\right) - - - - - - - - 2.2$$

In this relation, D_o is the temperature independent preexponential (m^2/s), Q is the activation energy for diffusion (J/mol or eV/atom), R is the gas constant, 8.31 J/mol.K or 8.62 x 10^{-5} eV/atom.K[18], [31].

In a cyaniding process, Brandt reported that carbon and nitrogen atoms penetrate the surface of steel rapidly. The penetration depth in the first 30 mins is 0.25 mm. This actually depends on the concentration of the pack cyanide and the type of steel[20].

2.7 Theory of Wear and Wear Experimentation

Wear is the progressive damage, involving material loss, which occurs on the surface of a component as a result of its motion relative to the adjacent working parts; it is the almost inevitable companion of friction[4].

Most tribological pairs are supplied with a lubricant as much to avoid the excessive wear and damage which would be present if the two surfaces were allowed to rub together dry as it is to reduce their frictional resistance to motion[4].

The economic consequences of wear are widespread and pervasive; they involve not only the costs of replacement parts, but also the expenses involved with machine downtime, lost production, and the consequent loss of business opportunities. Other side effects are decreased efficiency of worn plant and equipment leading to low performance and high energy consumption[4].

Wear occurs in many different scenarios, widely varying the conditions of wear. Solutions to these varieties of wear problems depend on identifying the specific nature of the wear in question. Tribological systems are used to determine the various parameters of wear. By varying these parameters, the wear mechanism of the wear is studied.

Figure 2-5: A pin-on-disc tribometer at AUST, Abuja – Nigeria.

The pin-on-disc tribometer helps to determine the material removal during the sliding of a pin on a disc of both standard dimensions. The pin with a hemispherical tip slides over a flat rotating circular disc.

Figure 2-6: Sample of pin.

The equipment does help to record coefficient of friction, frictional force and rotation count amongst other things. The coefficient of friction, μ is usually measured as a means of understanding some mechanism of wear. The coefficient of friction, μ relates to frictional force F_f, recorded during wear experiment, and normal force F_n, applied on the pin with the following equation[32]:

$$\mu = \frac{F_f}{F_n} - - - - - - - - 2.3$$

The amount of wear is determined by measuring approximate linear dimensions or weights both before and after each stage of the test. The resultant wear results are usually obtained by conducting the test over varying sliding distances for selected values of loads and sliding speeds[33]. When the hardness of both surfaces are not wide apart, the reasonable option is to utilize hard abrasive papers, made of SiC for instance, to obtain considerable wear volume.

The amount of wear in any system would depend on a number of factors. These factors include applied load, machine characteristics, sliding speed and distance, environmental conditions and the material properties[33]. The diagram below shows the operation of the tribometer.

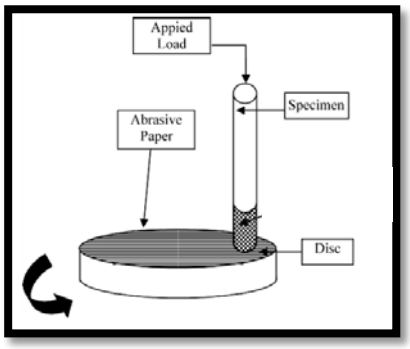

Figure 2-7: The abrasive wearing process[22].

Wearing of steel may be mild or severe. The resulting surface features helps in distinguishing between both types of wear. However, wear can be caused by melting, by oxidation, by corrosion, by delamination, by adhesion, by abrasion and by other phenomenon. The starting point of investigating wear rate, w of any metal is the use of the conventional and universal Archard wear equation, which is expressed through the relation:

$$w = K \times \frac{W}{H} - - - - - - - - 2.4$$

Where W is the load on the contact, H is the surface hardness, and K is the wear coefficient[4]. This equation has been transformed into different forms to fit various applications during wear experiments. One of those transformations is shown in the following relation:

$$w = \frac{K}{H} pv - - - - - - - - 2.5$$

Where v is the sliding speed, p is the applied pressure, H is the hardness of the softer material (brass in the simulations reported subsequently), and K is the wear coefficient, a constant which ranges from 10^{-3} to 10^{-7} W/mK for typical materials systems. In this case, the wear rate is measured in terms of height loss per unit time[34].

When abrasion rate, w in terms of volume loss (in mm cube) per Newton-meter is desired, the following relation is used:

$$w = \frac{\Delta G}{dMS} \left(\frac{mm^3}{Nm}\right) - - - - - - - - 2.6$$

Where ΔG is the mass loss, d is the density of the steel, M is the applied load, and S is the sliding distance[22], [35]–[37]. With these formulae, the weight loss and wear rate can be plotted against sliding distances as well as load. Further analysis of the wear mechanism responsible for the wearing behaviour is further explained in chapter 4 of results and discussion.

3.0 Materials and Methods

3.1 Sample Preparation

3.1.1 Preparation of Steel Sample

Nine cylindrical pins were machined; five from the new pickax and four from the used pickax. Each pin was about 50 mm in height with varying diameters along the height. At the top, the average diameter is about 12.6 mm spanning for 27.5 mm average height. Whereas at the bottom, the diameter is about 6.2 mm covering average height of 20 mm (see Fig 3-4a). In addition, the tips of the pins were shaped hemispherically with an average radius of 2.5 mm. The chemical compositions of the pins showed that the new and old pickaxes were made of AISI 1065 and 1070 carbon steels respectively. This analysis was done with Optical Emission Spectrometer (Solaris CCD Plus) made by GNR Analytical Instruments Group, Italy. Their respective average hardness were 281 and 275 VHN. These results are presented in Table 4-1 – 4-3 in Chapter 4 of "Results and Discussion".

As-received steel samples from two "Champion" pickaxes were prepared by cutting, milling and polishing into 9 pins of various sizes (See Figs 3-1 – 3-4).

Figure 3-1 a & b: New "Champion" pickax (left) and the metal head of a used "Champion" pickax (right) used for analysis in this research.

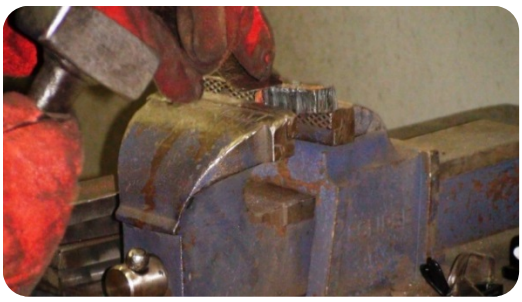

Figure 3-2 a & b: Cutting and shaping samples using an anvil device, electric saw and hammer (left); and using a band saw (right) at SCC Pipe Yard, Abuja – Nigeria.

Figure 3-3: Using the milling machine to prepare samples at SCC Pipe Yard, Abuja – Nigeria.

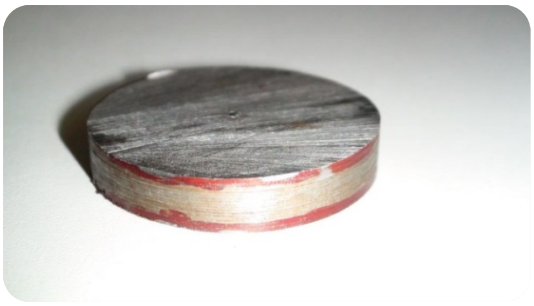

Figure 3-4 a & b: Pins machined from the pickaxes (left); Disc made of steel for wear experiment (right) at SCC Pipe Yard, Abuja – Nigeria.

9 disc samples (44 mm by 6 mm) were cut to serve as a base upon which SiC papers with 120 grit size were placed to serve as the abrasive material with higher hardness to wear off the surfaces of the pins as they slide over them (see Fig 3-4b).

3.1.2. Preparation of Cyanide Materials

Manihot esculenta, a local bitter cassava leaf specie, was used for the production of processed cyanide powder – containing considerable amounts of carbon and nitrogen. The cassava leaves were harvested from eight-month-old cassava plants at a farm near Engineering Materials Development Institute (EMDI), Akure, Ondo State, Nigeria. These leaves were then sun-dried for 4 days to reduce the moisture content and then pulverized into powder. The powder obtained was sieved to approximately $212 \pm 5\ \mu m$ particle size using an Octagon sieve shaker. 8:2 volume ratio, representing processed cassava leaf (PCL) to $BaCO_3$ was mixed and used for the pack cyaniding process. The $BaCO_3$ served as an energizer to activate and foster the process of diffusion of carbon into the surface of the metals.

3.2 Pack Cyaniding Procedure

Of the (nine) 9 pin samples, one (1) was untreated – meant to serve as control for the treated samples. Whereas, eight (8) were utilized for the pack cyaniding process – four (4) each from the 1065 and 1070 steels. The samples were completely embedded in the 8:2 PCL/$BaCO_3$ powder mixture within cyaniding boats (70 x 80 x 100 mm^3) (Fig 3-5a).

Figure 3-5 a & b: Steel pins in the pulverized cyanide pack and heat-treated.

Each of the boats was covered with a steel lid and sealed with fire clay to reduce escape of gaseous carbon and nitrogen from the boat during the heat treatment process. They were heat treated at four different temperatures, namely 750, 800, 850 and 900^{o}C for 5 hrs. All the batches were treated in a Thermolyne furnace of 1000^{o}C capacity at AUST Lab, Abuja – Nigeria (see Fig 3-5). After the treatment duration has been attained, the AISI 1065 steel samples from the new pickax were quenched rapidly with water, and then tempered to 300^{o}C for 3 hours; whereas, the AISI 1070 steel samples were air-cooled.

During the pack cyaniding treatment, rectangular samples (50 mm x 10 mm x 10 mm) were treated together with the pin samples under same conditions for metallographic examinations (see Fig 3-6).

Figure 3-6: Rectangular sample for metallographic examinations.

After pack cyaniding, each of the metallographic samples were polished and grounded with SiC abrasive papers for examinations.

3.3 Vickers Hardness Measurement

The surface hardness and case hardness profiles of pack cyanided 1065 and 1070 steel samples were measured using Micro-hardness tester on the sectioned pins. The hardness was measured base on three measurements using a load of 10kg (98N), with load time of 10s through a diamond pyramid indenter at the polished surface of each sample. The average hardness of the untreated pins of AISI 1065 and 1070 steel samples were 281 and 275 VHN respectively. Also, the hardness of the pack cyanided pin samples were measured and recorded as well. The hardness results are summarized in Table 4-4 and 4-5 of chapter 4.

3.4 Charpy Impact Test Procedure

Four (4) Charpy samples (two from both 1065 and 1070 steels, Fig 3-7a) were machined to verify the impact of increased hardness on the toughness of the carbonitrided samples. The samples were notched accordingly with the equipment shown in Fig 3-7b below. Two, per set were tested before and after the 850^{o}C pack cyaniding process. The Charpy impact test was carried out with the equipment shown in Fig 3-8 below.

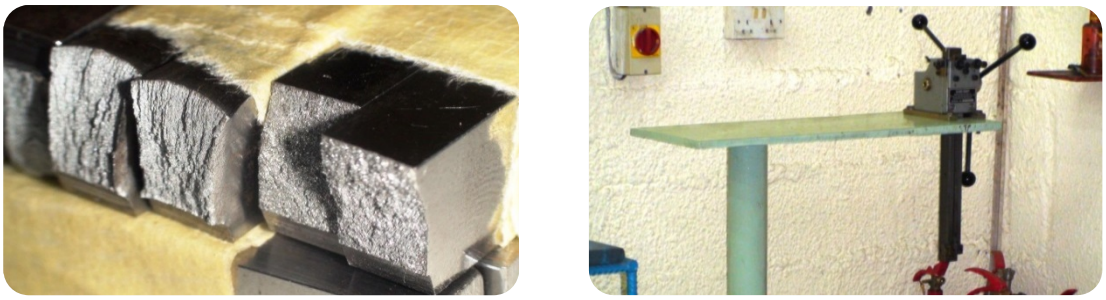

Figure 3-7a & b: Charpy samples (left). Equipment used to V-notch samples to 2mm depth and 45° angle (right) at SCC Pipe Yard, Abuja – Nigeria.

Figure 3-8: Charpy impact equipment at SCC Pipe Yard, Abuja – Nigeria.

3.5 Wear Test and Analysis Method

Abrasive wear tests of the pack cyanided and untreated AISI 1065 and 1070 steel specimens were carried out on a pin-on-disc wear testing machine which contained a fractional transducer to record the wear data under unlubricated condition at ambient temperature (25^{o}C) (Fig 3-9a, b & c). The SiC papers, upon which the pins glided over, were fixed on the discs with diameters ~44 mm and thickness of ~6 mm.

Figure 3-9a, b & c: Wearing of pin on SiC grit paper.

Before the test, the untreated and pack cyanided 1065 and 1070 steel pins were cleaned up with acetone – this was to remove debris adhering to the surface. The pin-on-disc test was carried out using the parameters in Table 3-1.

Table 3-1: Wear test parameters.

Parameter	Value
Speed of rotation	183.0 rpm
Sliding velocity	0.25 m/s
Applied load	10 N
Radius of wear track	13 mm
Max duration of each test	10.0 minutes
Time Intervals	2.0 minutes
Total sliding distance	150 m

In order to quantify the amount of material removed during the tests, each sample was weighed before and after the tests using an electronic balance with sensitivity of 10^{-5} at Sheda Science Complex, SHETSCO – Abuja (Figure 3-10). The weight losses of all the samples were determined at 2 min interval for the total of 10 min. The data for weight loss after each 2 min time interval were used for the analysis of wear rate of the worn surfaces. The wear resistances of the tested samples were evaluated, using sliding velocity of 0.25 m/s, constant normal load of 10 N and total sliding distance of 150 m. After each wear tests, the worn surfaces of the samples were examined by optical microscope – details of which are shown in chapter 4 of this report.

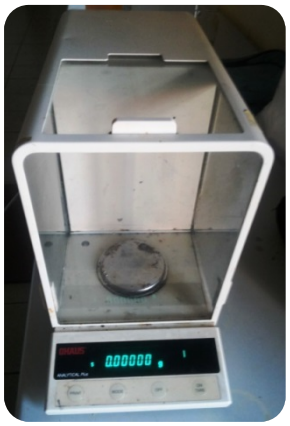

Figure 3-10: Electronic weighing balance with 10-5 sensitiveness at Sheda Science Complex, SHETSCO – Abuja.

4.0 Results and Discussion

4.1 Chemical Composition of As-Machined Samples

The appendix section displayed the detailed chemical analysis of the pickax samples, characterized at SCC Pipe Yard – Lab Section, Bwari – Abuja, Nigeria. These results, summarized for both the new and the used pickax are shown below:

Table 4-1: Chemical composition for a type of 1065, very-low alloy steel (signifying the new pickax).

Fe%	C%	Mn%	Si%	Cr%	Ni%	Ti%	W%	Co%	N%	P%	S%
98.222	0.616	0.724	0.188	0.048	0.032	0.009	0.007	0.006	0.044	0.029	0.015

Table 4-2: Chemical composition for a type of 1070, very-low alloy steel (signifying the used pickax).

Fe%	C%	Mn%	Si%	Cr%	Ni%	Ti%	W%	Co%	N%	P%	S%
98.014	0.749	0.968	0.142	0.019	<0.002	0.011	0.008	0.002	0.033	0.024	0.006

Both steels are called types of 1065 and 1070 carbon steels because their carbon and manganese content falls within that classification of the American Iron and Steel Institute (AISI). Ideally, 1065 and 1070 steel does not contain other alloying elements as shown in tables 4.1 and 4.2. These other alloys are in minute quantities, such that they do not fall within any other classification whatsoever. They however, contribute to the results of the steels' hardness. This would be discussed in a later section.

Meanwhile, some observations are noted. First, both molybdenum contents are too low (<0.002) – reason for excluding it from tables 4-1 and 4-2. Also, phosphorous and sulphur are within acceptable limits of 0.04 max and 0.05 max respectively[11].

4.2 Microstructural Analysis

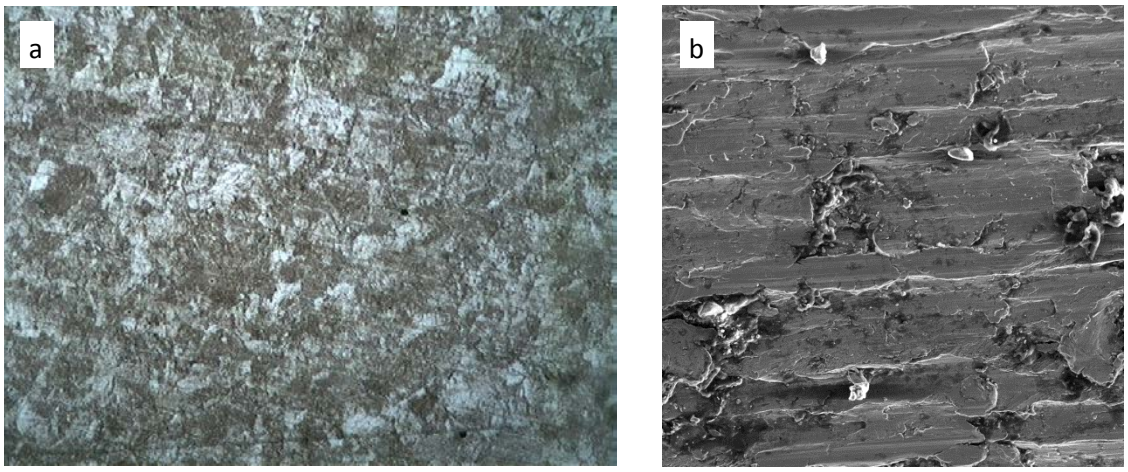

Figure 4-1: Micrographs of 1065 proeutectoid steel a) Optical image at 100x showing the proeutectoid ferrite (white) and pearlite (dark) phases. b) SEM image at 500x showing the pearlite with the cementite and ferrite lamela structure.

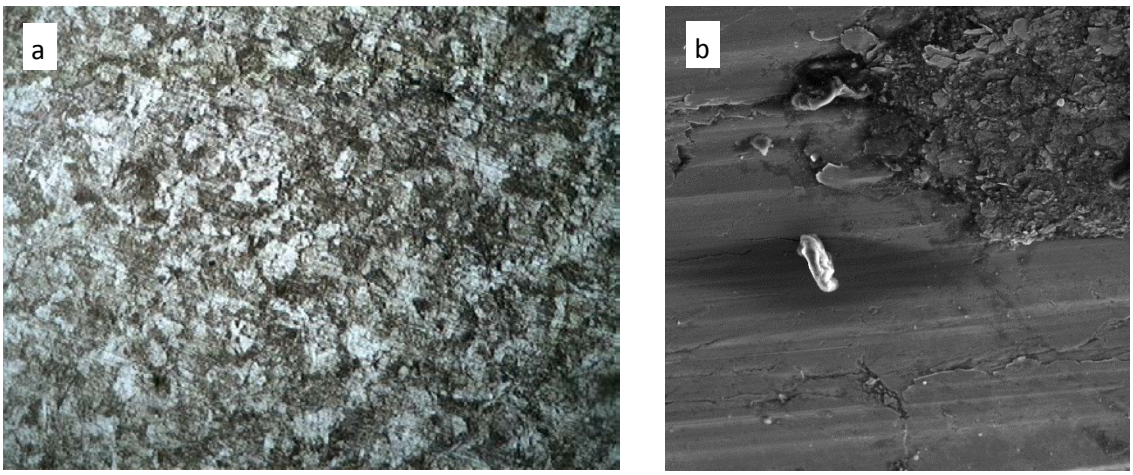

Figure 4-2: Micrographs of 1070 proeutectoid steel a) Optical image at 100x showing the proeutectoid ferrite (white) and pearlite (dark) phases. b) SEM image at 500x showing the predominance of ferrite phase.

The ferrite phase of the 1070 steel is more predominant than that of the 1065. This is one possible reason for the lower hardness measurement of 1070 as against that of the 1065, as the ferrite phase is generally not as hard as the cementite phase.

4.3 Hardness of 1065 and 1070 Steels

4.3.1 Hardness Difference of the As-Machined Steels

Table 4-3: Vickers hardness of as-received 1065 and 1070, carbon steel.

	Vickers Hardness, HV			
	Point 1	Point 2	Point 3	Average
As-Machined 1065	289	286	269	**281**
As-Machined 1070	277	276	271	**275**

The difference in the higher hardness value of the as-received 1065 steel over that of 1070 steel are principally due to two phenomena, namely: their chemical compositions and microstructure.

Higher carbon and manganese content is expected to offer higher hardness and strength. On this basis, the as-received 1070 steel should be harder than the as-received 1065 steel (See Tables 4-1 and 4-2). However, that is not the case. The balance of higher chromium, nickel and nitrogen contents in the 1065 steel makes it harder than the 1070 steel. The difference for the titanium and tungsten are not so wide apart to create significant impact. Cobalt in the 1065 steel (0.006%) increases the rate of nucleation and growth of pearlite, and hence decreases the hardenability of the steel compared to that of 1070 steel (0.002%). The difference in the cobalt content is equally not significant enough to cause major hardening loss.

In addition, the microstructures as shown in 4.2 further confirm the basis for the increased hardness of the 1065 over that of 1070 steel. The larger widespread of the ferrite phase in the 1070 steel, having lesser hardness value is responsible for this.

4.3.2 Vickers Hardness of the Carbonitrided Steels

The tables and charts below show the Vickers hardness for the as-received and carbonitrided 1065 and 1070 steels. Generally, the hardness of the quenched and tempered carbonitrided 1065 steel demonstrates higher hardness than those of the air-cooled 1070 type steels (more on this in later sections).

Table 4-4: Hardness values for as-received and carbonitrided 1065 steel.

Carbonitrided Temperature	**Vickers Hardness, HV**			
	Point 1	Point 2	Point 3	Average
As-Received	289	286	269	**281**
750°C	361	323	318	**334**
800°C	438	436	349	**408**
850°C	554	546	526	**542**
900°C	712	705	701	**706**

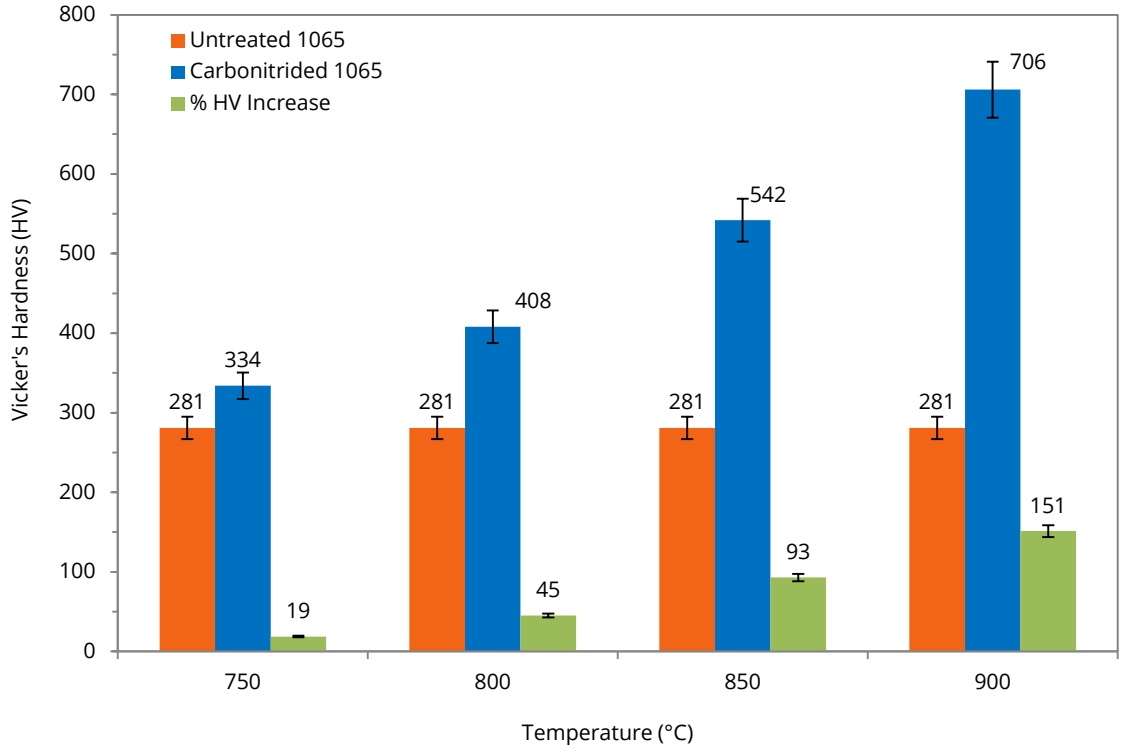

Figure 4-3: Hardness Vs Temperature for AISI 1065 Steel, Water Quenched and Tempered at 300°C.

Table 4-5: Hardness values for as-received and carbonitrided 1070 steel.

Carbonitrided Temperature	Vickers Hardness, HV			
	Point 1	Point 2	Point 3	Average
As-Received	277	276	271	**275**
750°C	286	286	267	**280**
800°C	313	299	284	**299**
850°C	350	332	313	**332**
900°C	362	355	351	**356**

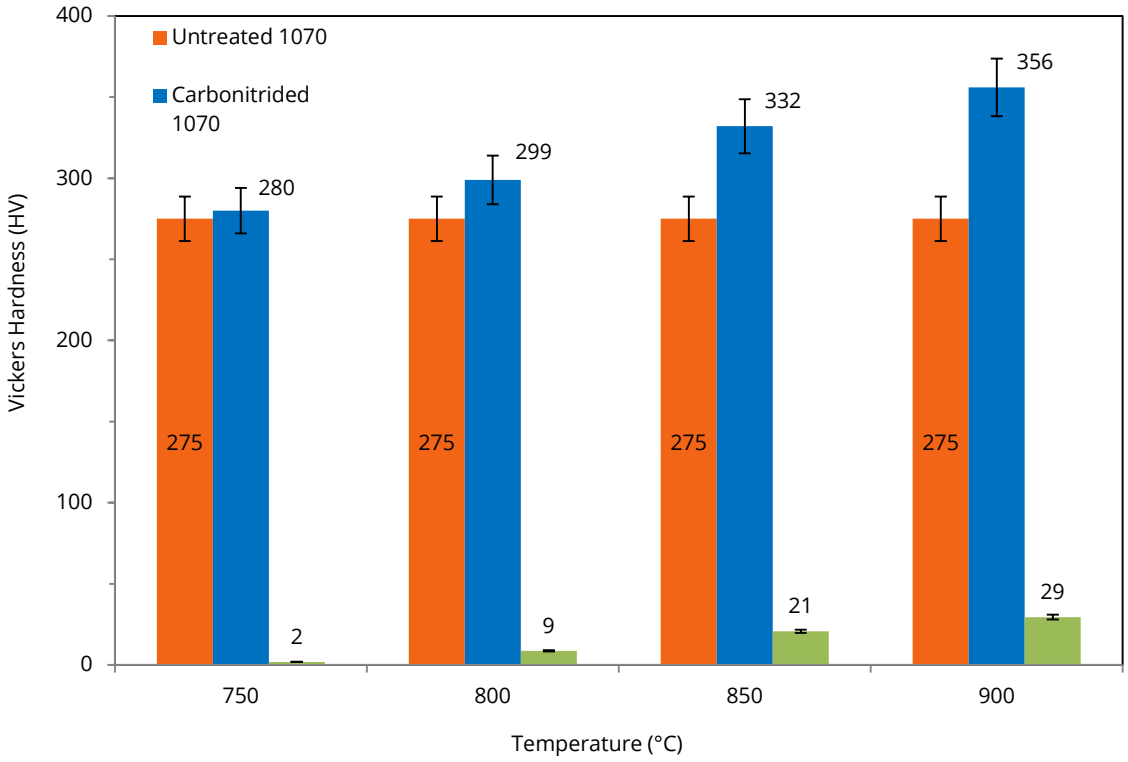

Figure 4-4: Hardness Vs Temperature for AISI 1070 Steel, Air Cooled.

4.3.3 Surface Hardening by Diffusion of Carbon and Nitrogen

The carbon interstitially diffused into the surface of the steel at the austenitic temperature (or upper transformation temperature, [Ac1]), where there is appreciable interstitial solid solubility of carbon in austenite. This was the basis for commencing the carbonitriding temperature from 750°C, even though 790°C is the minimum temperature recommended for carburizing. Actually, the most preferred

ranges are between 850 – 950°C[11]. The results of the wear rate and coefficient of friction to be presented in the following sections would show the significance of this recommendation. At 850 to 950°C, carbon diffuses better and increases the hardness in such a way that offers reduced wear rates over lower or higher temperatures (more on this in following sessions).

Likewise, nitrogen diffuses sufficiently into the interstitial spaces and equally increases hardness, but at relatively lower temperatures. The ideal temperature range for this diffusion was not studied in this research. It is however subject to further investigation. Meanwhile, the hardness result obtained showed that the solubility of carbon in the Fe-C alloy increased with increasing temperature. Chemical analysis of the resultant carbonitrided steel would further buttress this point. However, the hardness profile of both steels, shown in Figs 4.5 and 4.6, demonstrate the presence of increased carbides and nitrides at the surface than that towards the core of the material. This is responsible for the increased hardness at the, or towards the surface. The alternating harness in the towards the core of the 1070 air cooled steel is due to varying hardness values of the pearlite steel formed with varying layers of cementite (hard) and ferrite (soft) phases.

The presence of nitrides in the steel as a result diffused nitrogen contributed to the increased hardenability of the steel. The diffused nitrogen also performs another function. It stabilizes the austenitic phase resulting in retained austenite, particularly in the steel with very low alloy compositions.

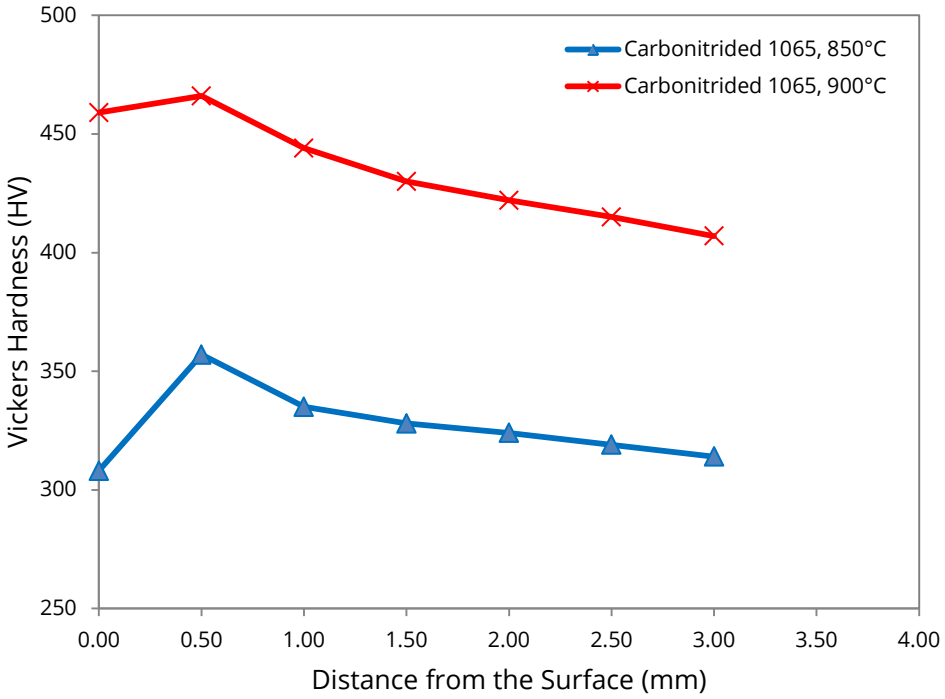

Figure 4-5: Hardness Distribution of the 1065 Steel Carbonitrided for 5hrs at 850 & 900°C, Water Quenched and Tempered at 300°C for 3hrs.

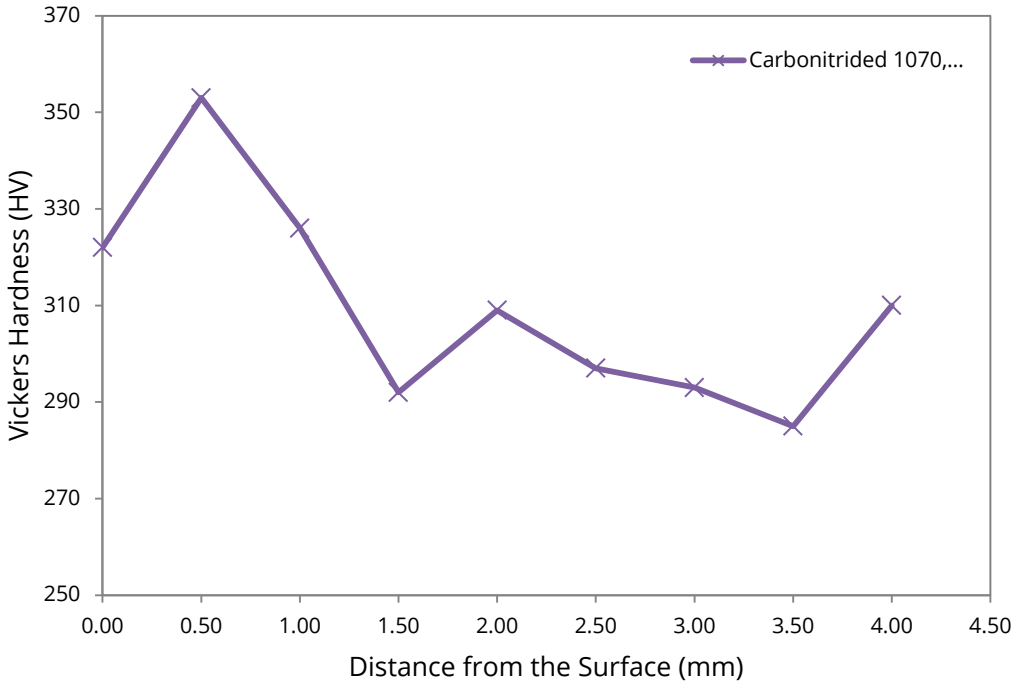

Figure 4-6: Hardness Distribution of the 1065 Steel Carbonitrided for 5hrs at 750, 800, 850 & 900°C, Water Quenched and Tempered at 300°C for 3hrs.

When the austenite phase of steel is stabilized, it means that the eutectoid temperature is reduced[38]. Hence, stabilizing the austenitic phase allows the steel to retain the interstitial carbon and nitrogen at lower/room temperatures, giving the steel an austenitic microstructure with a hardened composition. The austenite stabilizing elements in the chemical composition of the 1065 and 1070 type high-carbon very low alloy steels include manganese and nickel. However, the presence of ferrite-stabilizing elements, like silicon and chromium formed carbides during heat treatment, and hence shifts the eutectoid temperature to higher values. This therefore reduces the austenitic phase and introduced the ferrite-phase, thereby giving rise to an ausferrite microstructure.

4.3.4 Hardenability Induced by Quenching and Tempering 1065 Steel

The hardenability of the carbonitrided 1065 steel, quenched in water to room temperature, and tempered at 300°C for 3hours is higher than those of air cooled 1070 steel as seen from Fig 4.3 to 4.6. This is due to the martensitic phase formed by preventing the escape of carbon from the steel upon cooling from the austenitic phase. This is unlike the alternating, but lesser hardness of the ferritic and cementite phases formed in the air cooled 1070 steels. The resultant martensitic transformations, wherein a metastable phase is produced gives the 1065 steel higher hardness values over those of the 1070 steel. Further microscopic and chemical

studies of their respective diffusionless and diffusion-dependent transformations would buttress this point.

Meanwhile, this transformation involves two stages. Large number of atoms, in the first phase experiences slight displacement of each atom relative to their neighbors. The resultant body centered tetragonal (BCT) martensite, transformed polymorphically from the FCC austenite, retains all the carbon and nitrogen impurities at the interstitial sites, giving it a supersaturated state, capable of transforming upon further heating[31]. The trapped carbon and nitrogen atoms effectively hinder dislocation motion as well as the BCT structure that offers relatively fewer slip systems along which dislocation moves. Hence, when the surface of the steel is indented or scratched, it experiences higher resistance to deformation, making the trapped atoms and the BCT structure the principal basis for the increased hardness and strength of martensitic steels. Although the hardest and strongest, martensitic steels have been known to exhibit the least toughness. This is why they are usually tempered to relax the stresses present and improve the toughness.

The tempering (second) stage transforms this BCT single phase structure into alpha ferrite and cementite phases. Unlike the pearlite, the microstructure is like that of a spheroidite, but with smaller cementite grains that had nucleated and grown in a ferrite matrix phase. The cementite, having higher hardness and strength, reinforces the ferrite phase at the grain boundary. It does this by increasing its resistance to dislocation motion. The ferrite phase improves the toughness, making tempered martensitic steels more ductile than martensitic steels. The drop in toughness of the

1065 steel is anomalous, but has an explanation as to why that happened. This drop is due to one-step embrittlement (more on this later).

In addition, the low alloys present in the steel increases hardenability and allows slow quench rates, thereby giving rise to less distortion and less tendencies to crack during quenching[11]. The depth and distribution of hardening upon quenching from austenite region is the basis for case hardening of steels. This is seen in Figs 4.5 and 4.6 above.

4.3.5 Increase in Hardness as a Result of Cooling by Air

The hardenability of the air-cooled carbonitrided 1070 steel is principally due to the increased carbon and nitrogen. The microstructure is expected not to change much as the transformation from the austenite phase to the alpha-ferrite and cementite phase still persists. The only difference is that the steel may no more be a eutectoid steel depending on the amount of carbon atoms added. It is expected to be a hypo-eutectoid steel as more carbon atom has diffused into the steel. Microscopic images and chemical analysis of the carbonitrided steel would further validate this claim.

4.3.6 Comparison of Hardness Result with Literature

The hardness value of 1850 by Tabur et. al., 2009 in table 4.5 was principally due to the formation of iron borides at the surface of the metal. Boron has been known to form very hard surface layers with metals. The only setback is the cost of purchasing boron for this operation. Also, the environmental hazard of boronizing is quite high.

Also, the hardness of 1512 HV by Abdul-Azis et. al., 2012 demonstrates impressive result. The varying variable was the pressure at which the carburization process was carried out. At 74MPa, carbon was introduced into the surface of the metal at a maximum case depth of 64μm. The influence of pressure played a great role in the process; however, the cost of executing this process is equally high, especially with the purchase of carburizing gas.

Table 4-6: Comparison between Vickers hardness of current work and literature.

Work	Media	Steel	Temp (°C)	Duration	HV
Tabur et. al., 2009	Pack-Boronizing	8620	950°C	6 hrs	1850
Abdul-Azis et. al., 2012	Pressurized Carburization	DSS Stainless	950°C	4 hrs	1512
Ibironke et. al., 2004	Pack-Cyaniding	Mild	860°C	4 hrs	540
Current work, 2014	Pack-Cyaniding	1065	900°C	5 hrs	**706**

Iborinke et. al. 2004 first conducted pack-cyaniding for the first time using cassava leaves. The maximum Vickers hardness result obtained was 540.02 HV. This was at a

temperature of 860°C for 4 hours. This breakthrough research was phenomenal as it paved way for further works in this area. Be that as it may, cyaniding at 900°C for 5 hours gave a better result as shown in table 4.5. The only variable is the chemical compositions of the various steels used, which does play crucial role in the mechanical behaviour of the treated metal. However, with an increase of 706 HV from 540 HV, it is a considerable improvement in that pioneer work.

In addition, the use of waste – cassava leaves for improving hardness of metals saves cost and is environmentally friendly.

4.4 Toughness of 1065 and 1070 Type Steel

The Charpy impact results for the toughness values of the 1065 and the 1070 steels are as shown in tables 4.6 and 4.7.

Table 4-7: Impact Test Result for As-received 1065 and 1070 Type Steel.

Specimen	Width (mm)	Thickness (mm)	Section (mm^2)	**Energy (J)**	**Modulus of Resilience, Ur (MJ/m^3)**	LE (mm)
1065 Type	6	10	60	**3.1**	**5.167**	0.6
1070 Type	6	10	60	**2.0**	**3.33**	0.69

Table 4-8: Impact Test Result for Carbonitrided 1065 and 1070 Type Steel.

Specimen	Width (mm)	Thickness (mm)	Section (mm^2)	**Energy (J)**	**Modulus of Resilience, Ur (MJ/m^3)**	LE (mm)
1065 Type	6	10	60	**2.4**	**4.00**	0.45
1070 Type	6	10	60	**1.5**	**2.5**	0.59

The energy to fracture and the linear extension of the fractured Charpy pins are shown above in tables 4.7 and 4.8. Their respective modulus of resilience were equally measured, but converted into the shown units. From these results, there was a considerable drop on energy, by a difference of 0.7J for the 1065 steel and 0.5J for the 1070 steel. This difference shows that the toughness of tempered martensite is less than slowly cooled steel. However, both steels were expected to have increased in toughness.

Commercial high-strength low-alloy steels with quenched and tempered martensitic microstructures usually display (one-step) tempered embrittlement at tempering temperatures of 200 to 370^{o}C[38]. This phenomenon occurred in this work with the anomalous decrease in the notched-bar energy from 3.1 to 2.4J and 2.0 to 1.5J as observed in the charpy impact test of the 300^{o}C tempered martensitic 1065 type steel and air-cooled 1070 type steel. The cause of this one-step embrittlement is attributed to four factors:

1. The precipitation of cementite from the retained austenite in the tempered martensite could not be retarded by the low alloys present, especially that of the silicon. *In quenched and tempered steel, with very low silicon contents, the retained austenite decomposes upon tempering at 300^{o}C to cementite films forming around the silicon. This reaction contributes to martensitic embrittlement.* Briant and Banerji 1978, showed from their experimental work that the anomalous drop in impact-energy coincides with the beginning of cementite precipitation[39].

2. Briant and Banerji 1978, also noted that intergranular mode of fracture along prior austenitic grain boundaries was proven by their experimental work to be caused by one-step embrittlement[39]. The segregation of phosphorus (0.029%), nitrogen (0.044%) and possibly sulphur (0.015%) to the austenitic grain boundaries is essential for this type of embrittlement leading to reduced toughness and transverse ductility. Although phosphorous and sulphur are within acceptable limits, they are usually kept as low as 0.015% to reduce this embrittlement[38].

3. Manganese, the secondary alloying element in this application, might have had an indirect contribution in fostering the segregation of phosphorous and sulphur to the grain boundaries[39].

4. Undissolved carbides, possibly present at the prior austenitic grain boundaries is thought to feature the impurity-induced intergranular fracture, as it acts as slip barriers[39].

Uncontrolled penetration of air into the furnace might have played a role in increasing the formation of oxide inclusions[40], which contributes to the decreased toughness of the steel. This however can only be validated by further investigation.

4.5 Strength of Carbonitrided 1065 and 1070 Steels

Unlike the toughness results, the 1065 steel experienced a slight increase in strength, while the 1070 did not. This is possible as the microstructures of both steels were altered. One alteration favored increase in the strength, the other did not. The calculation below depicts these strength differences.

For the 1065 steel, the Modulus of Resilience:

$$U_r = \frac{1}{2}\sigma_y\epsilon_y \rightarrow \sigma_y = \frac{2U_r}{\epsilon_y} - - - - - - 4.1$$

$$\epsilon_{y1} = \frac{0.6mm}{55mm} = \mathbf{0.0109};\ \ \epsilon_{y2} = \frac{0.45mm}{55mm} = \mathbf{0.00818}$$

$$\sigma_{y1} = \frac{2 \times 5.167 \times 10^6}{0.0109} = \mathbf{948\ MPa};\ \ \sigma_{y2} = \frac{2 \times 4.0 \times 10^6}{0.00818} = \mathbf{978\ MPa}$$

Where 1 refers to as-received sample and 2 is the tempered martensitic steel.

Notice the increase in yield strength from 948 to 979MPa. This difference in strength is due to the microstructure of the 1065 steel that was explained earlier. The strength values is validated by the strength of AISI 1060 steel, that was oil-quenched and tempered at 300°C. The values adapted from Ashby 2011 – CES EduPack 2011 ranges from 700 to 860 MPa[41].

For the 1070 steel, the Modulus of Resilience:

$$U_r = \frac{1}{2}\sigma_y\epsilon_y \rightarrow \sigma_y = \frac{2U_r}{\epsilon_y} - - - - - - 4.2$$

$$\epsilon_{y1} = \frac{0.69mm}{55mm} = \mathbf{0.01254};\ \ \epsilon_{y2} = \frac{0.60mm}{55mm} = \mathbf{0.01072}$$

$$\sigma_{y1} = \frac{2 \times 3.33 \times 10^6}{0.0109} = \mathbf{531\ MPa};\ \ \sigma_{y2} = \frac{2 \times 2.5 \times 10^6}{0.00818} = \mathbf{466\ MPa}$$

Where 1 refers to as-received sample and 2 is the tempered martensitic steel.

The reduced yield strength in the 1070 steel is not a desirable property. This drop is attributed to the pearlite microstructure that was formed after the carbonitriding process. Pearlite, known for lower strength due to the ferrite phase present has shown a drop in strength as more carbon and nitrogen atoms where diffused into the surface of the steel.

The hardness, toughness and strength of air-cooled steel are seen to be non-desirable as compared to the quenched and tempered steel. The ductility of the air-cooled steel is seen to be better as the difference with the yield strain is not that much. This difference is 0.00182 compared to 0.00272 of the tempered martensitic steel described earlier.

4.6 Pin-on-Disc Wear Results and Analysis

4.6.1 Defining the Dominant Wear Mechanism

The results of the wear experiments described in chapter 3 are compared with Lim and Ashby wear mechanism map. This was to establish the wear mechanism of the steels.

The first question to answer is what the underlying mechanism behind the wear of the steels over the SiC papers is? To answer this question, the wear mechanism map by Lim and Ashby 1987 is used to analyze the mechanism behind the wearing of the steel as XRD analysis of the worn debris could not be obtained at the time of this report.

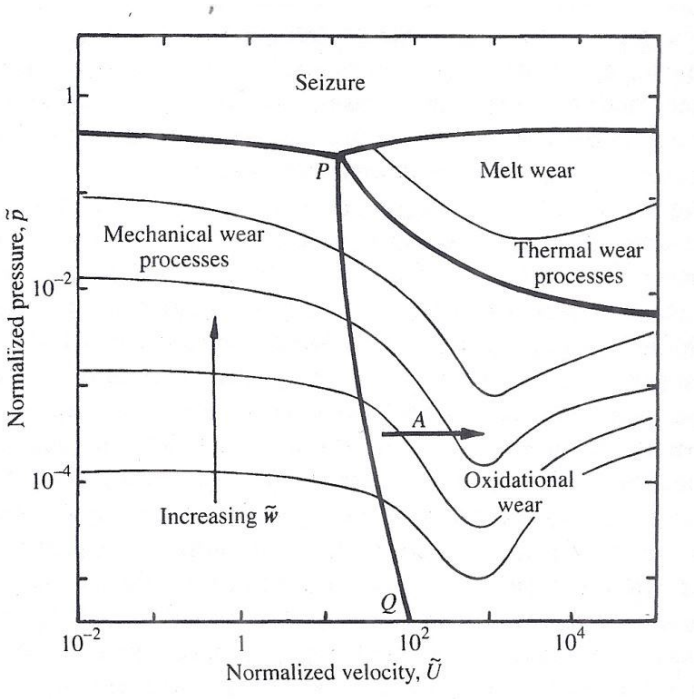

Figure 4-7: The essential features of a load-speed wear mechanism map for steel using a pin-on-disc configuration. Load and speed normalized using a set of formulae shown in the appendix section. Thick lines delineate different wear mechanisms and thin lines are contours of equal wear rate, w[4], [42].

From the calculations of normalized pressure and normalized velocity using experimental results, the plot on the wear map above, fell within the mechanical wear processes as shown in Fig 4.8. The results did not cross the transition point into the oxidative wear. The mark however, fell within the mechanical wear region. Note that the value of velocity to normalized velocity is 1m/s to 100[4], [42]. However the formula is in the appendix section.

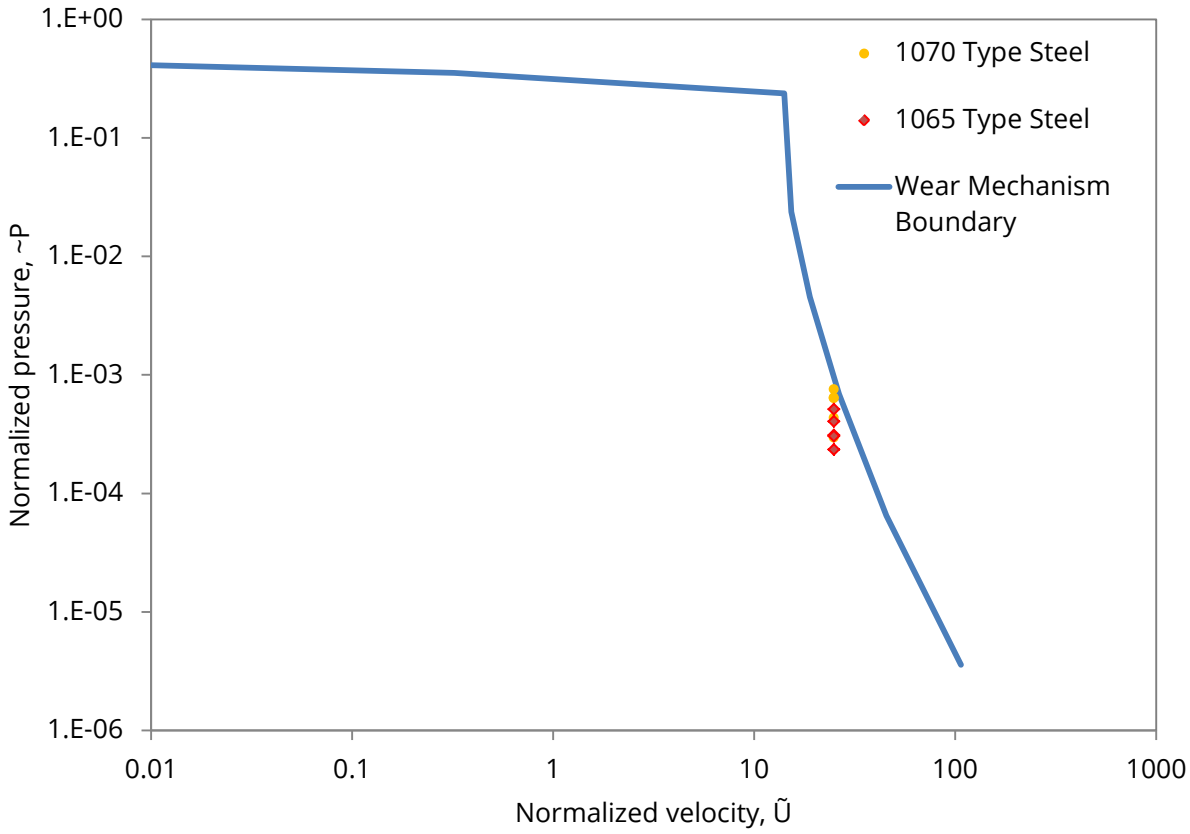

Figure 4-8: Plot of normalized pressure against normalized velocity of untreated and carbonitrided 1065 and 1070 type steel on Wear Map.

One of the wear values of the 1070 steel was at the verge of the oxidative wear. This shows a tendency for the initiation of oxidative wear in that metal during the wear experiment. But more profound is the increased rate of wear for the 1070 steel over those of the 1065 steel as shown above.

Abrasive wear lies within the mechanical wear domain. In this domain, the wear can be running-in, adhesive, delamination or abrasive[4]. However, it is not running-in because the operating conditions must be in a lubricating media, but our media in this case is dry sliding. It is equally not adhesive because the touching asperities did not adhere together as would have been expected, especially for similar rubbing materials. It would have been delamination if cracks nucleated at the wear surface of the pin and plastic shear deformation is induced at the softer surface. The wear mechanism is abrasive because the counterface, which is that of the silicon carbide (SiC), is both rough and harder than the wearing component, which is the pin.

Here are a few points to note:

1. Slow sliding results in comparatively low normal surface pressures. Hence increase in temperature is likely modest[4].
2. Since mechanism of wear has been demonstrated as mechanical, the debris is expected to be metal particles and not oxides of metals.

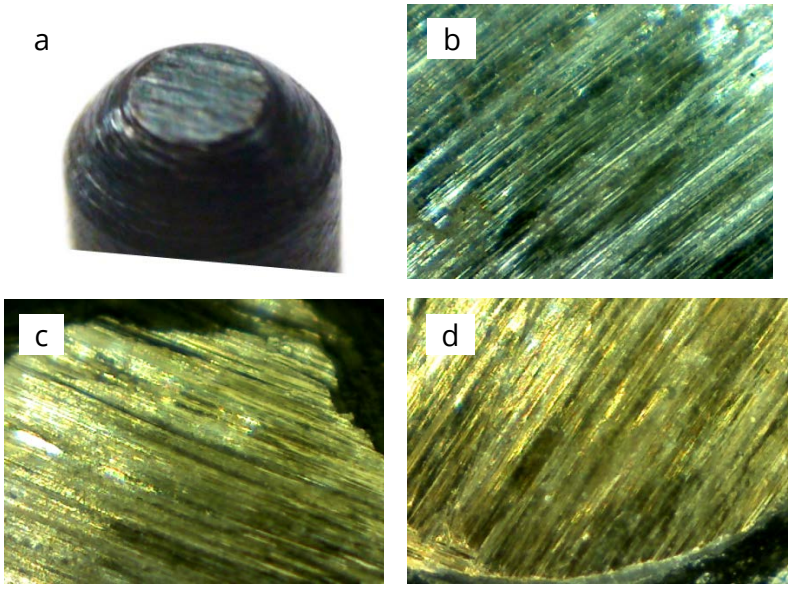

Figure 4-9: Optical micrographs of worn surfaces of 1065 type steel: a) camera image of surface, b) Untreated sample, c) 850°C sample, d) 900°C sample.

3. Optical micrographs shown above in Fig 4.9 further validates the claim that severe abrasive wear was obvious, as parallel grooves running in the rubbing direction were seen. In addition, the volume and size of the grooves varies form light scratching at one end to severe gouges at the other.

4.6.2 Wear Rate against Sliding Distance

The plot of wear rate against sliding distance of Fig 4-10 demonstrates a sharp increase at sliding distance of 30m (or 2mins) and sharp drop at 60m. This result is consistent with those obtained from literature using high abrasive papers as the counterface disc.

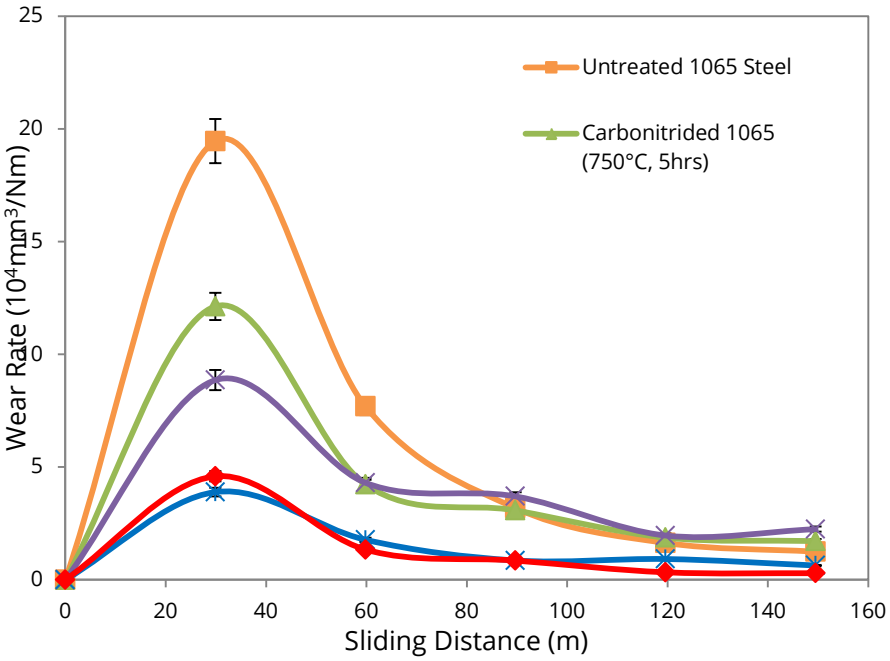

Figure 4-10: Variation of Wear Rate with Sliding Distance of AISI 1065 Steel, Carbonitrided (750°C, 800°C, 850°C, 900°C; 5hrs), Water-Quenched and Tempered (300°C, 3hrs).

The reason for this sharp increase and sharp drop in wear rate is due to the size and roughness of the counterface SiC papers. At first, the size and roughness of the SiC papers where high, but became increasingly diluted as worn particles of the pin accumulate over time on the surface of the paper. The combined debris from the pin and those from the abrasive paper reduced the roughness and consequently the wear rate as the sliding distance increased. The peak at 30m sliding distance was as a result of the initial roughness of the SiC paper which was quickly reduced by high volume of the worn pin particles.

The wear rates were lower for the carbonitriding at higher temperature values. The basis for this reduced hardness has been explained under the section on hardness. The volumes and precise compositions of the carbide and nitride phases present in all the steels would help to further explain this point. However, the surface of the hardened steel imposes great wear resistance relative to the carbonitrided temperatures than the untreated steel. Once the hardened surface was removed, the material returns to the untreated state – reason for the almost uniform wear rate at the end of 150m sliding distance. The difference still observed towards the final sliding distance is due to higher hardness of the case layer and the inner core of the sliding surface. The case layer imposes greater resistance than the core as a result of the case hardening that was done.

4.6.3 Weight Loss against Sliding Distance

The accumulated debris on the surface of the grit paper over increasing sliding distance play significant role in varying the amount of material that is removed. The untreated and carbonitrided (@ 900°C) 1065 steel follow the expected path.

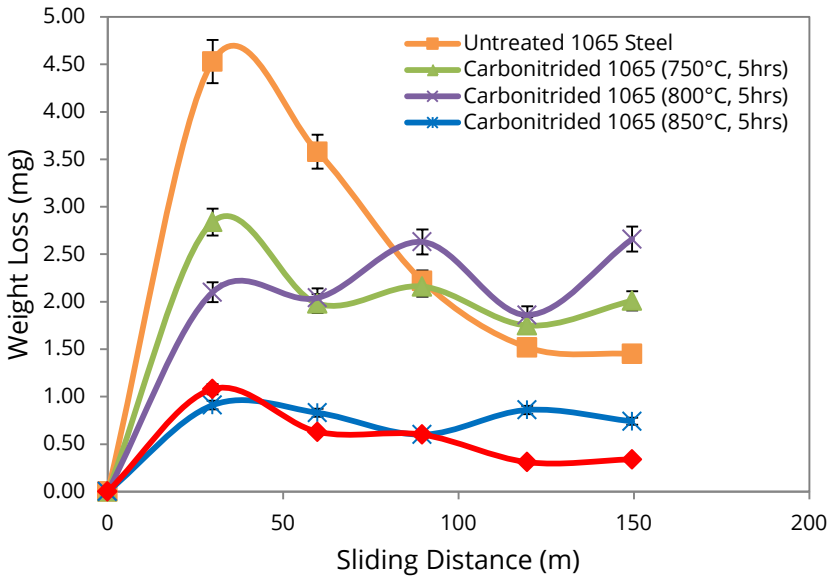

Figure 4-11: Variation of Weight Loss with Sliding Distance of AISI Steel, Carbonitrided (750°C, 800°C, 850°C, 900°C; 5hrs), Water-Quenched and Tempered (300°C, 3hrs).

The anomalies in others are best explained with graphs on coefficient of friction.

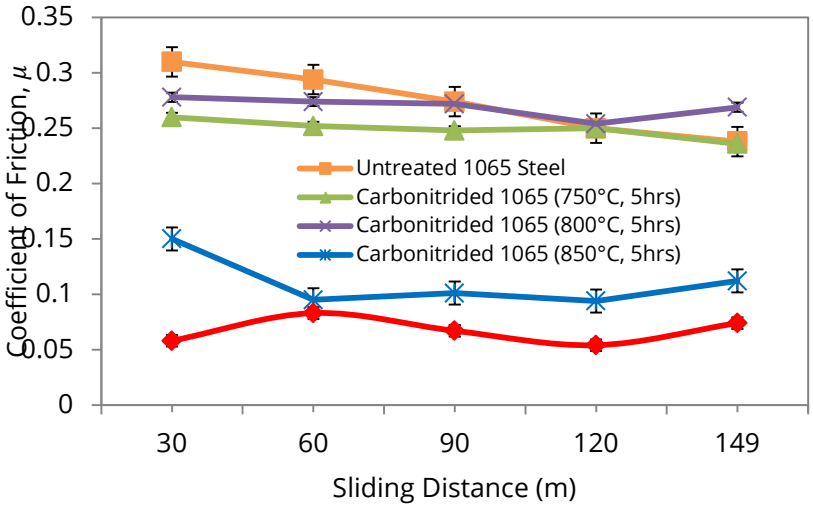

Figure 4-12: Coefficient of Friction Recorded Against Sliding Distance During Test of AISI 1065 Steel, Carbonitrided (750°C, 800°C, 850°C, 900°C; 5hrs), Water-Quenched and Tempered (300°C, 3hrs).

4.6.4 Coefficient of Friction against Sliding Distance and Wear Rates

From Fig 4.12, the weight losses of Fig 4.11 at successive sliding distances are closely related to their respective coefficients of friction. Higher coefficient of friction results in relatively higher weight loss and consequently higher wear rate, except for a few scenarios where other factors play crucial role. But generally, higher carbonitriding temperature results in lower wear rates. This delineation is clearly seen in Figs 4.12 and 4.13. This is due to the amount of carbon and nitrogen atoms that dissolved in the interstitial spaces, which consequently diffused upon tempering to create more cementite phase with smaller grain sizes. The higher the number of carbon, nitrogen and grain sizes the higher the resistance of the surface to wear and the lower the coefficient of friction.

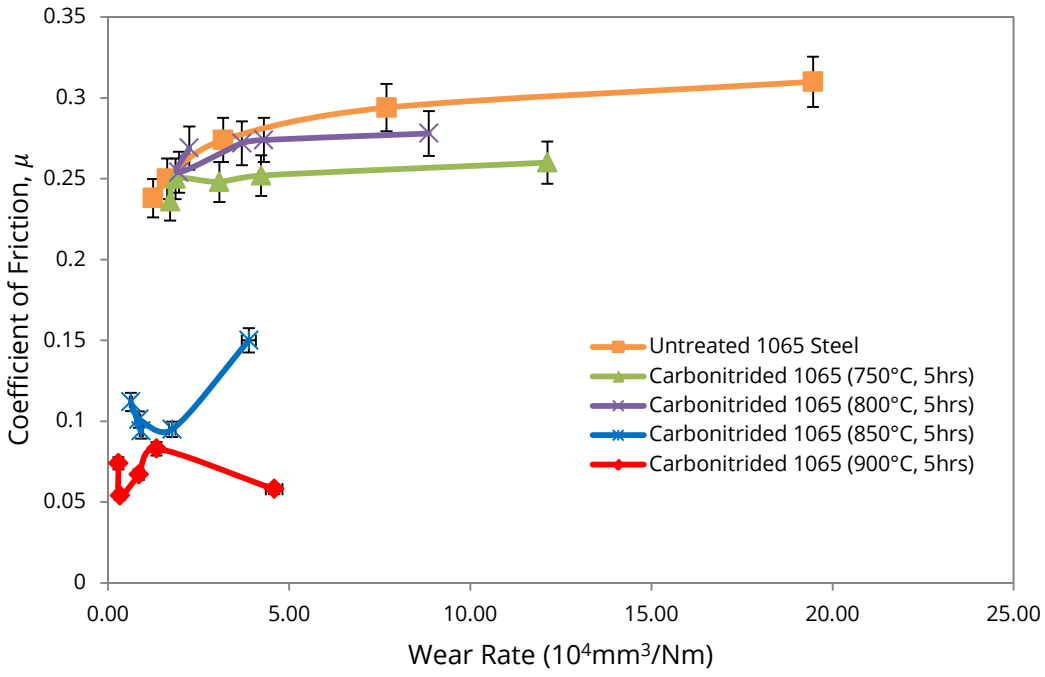

Figure 4-13: Variation of Wear Rate with Weight Loss of AISI 1065 Steel, Carbonitrided (750°C, 800°C, 850°C, 900°C; 5hrs), Water-Quenched and Tempered (300°C, 3hrs).

The initial drop for carbonitrided steels at 800, 850 and 950°C are due to the pile up of some of the worn materials on the abrasive silicon carbide paper in the form of curly slivers or chips, responsible in decreasing the surface roughness of the abrasive paper by introducing a third body in the system, which is a combination of some of the worn silicon carbide particles and wear debris from the softer steel. The precise amount, sizes and chemical composition of this debris are responsible for the varying wear rates and grooves on the surfaces of the steel.

4.6.5 Total Weight Loss against Hardness

For this application, material removal is a function of friction coefficient and hardness.

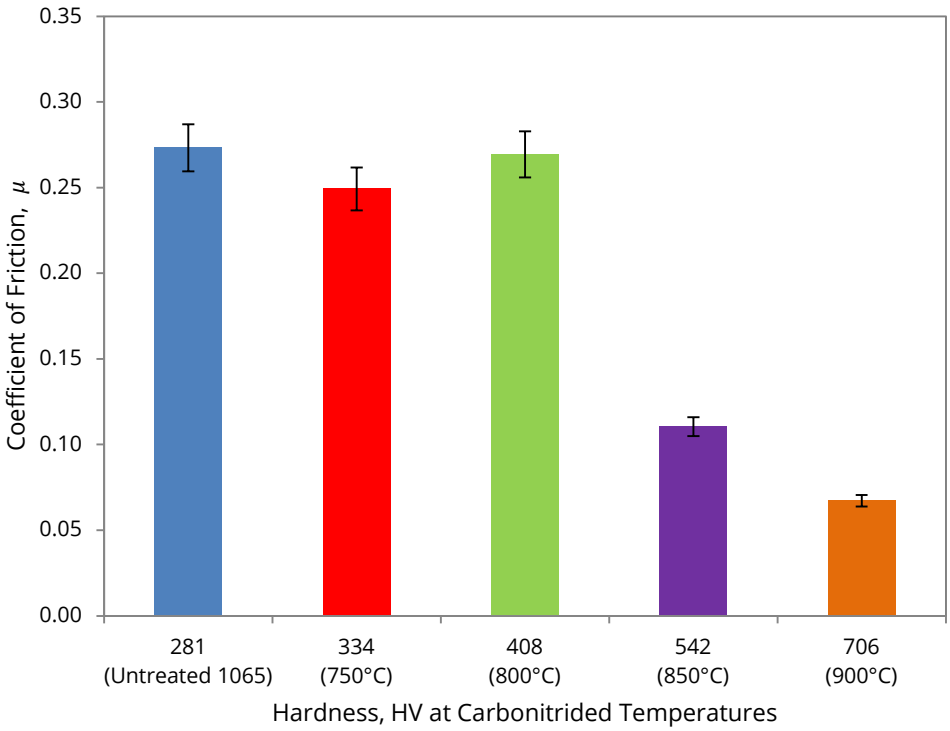

Figure 4-14: Coefficient of Friction against Varying Hardnesses of AISI 1065 Steel that was Carbonitrided at Different Temperatures for 5hrs, Water-Quenched and Tempered at 300C for 3hrs.

In other words, higher material removal imposes greater resistance and of course greater coefficient of friction. And since the plot shows that the material with the lower hardness experienced high wear removal at constant normal load, it is expected that the coefficient of friction would be higher. This is further demonstrated with the result of Fig 4.15, i.e. increasing hardness resulting in reduced weight loss. The anomaly for that of the steel carbonitrided at 750°C can best be explained with XRD analysis of the steel, except that some form of unnoticed error occurred during the wear experiment.

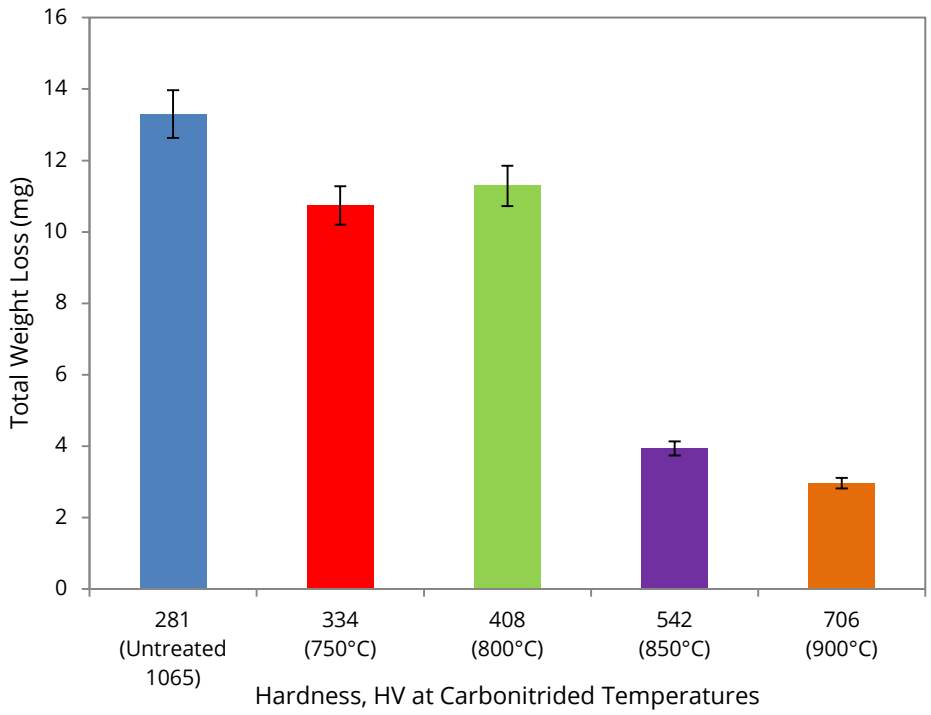

Figure 4-15: Total Weight Losses Against Varying Hardnesses of AISI 1065 Steel that was Carbonitrided at Different Temperatures for 5hrs, Water-Quenched and Tempered at 300C for 3hrs.

However, this anomaly does not distort the average wear rate values against the hardness of steels which validates the fact that increased hardness results in decreased wear rate as shown in Fig 4-16.

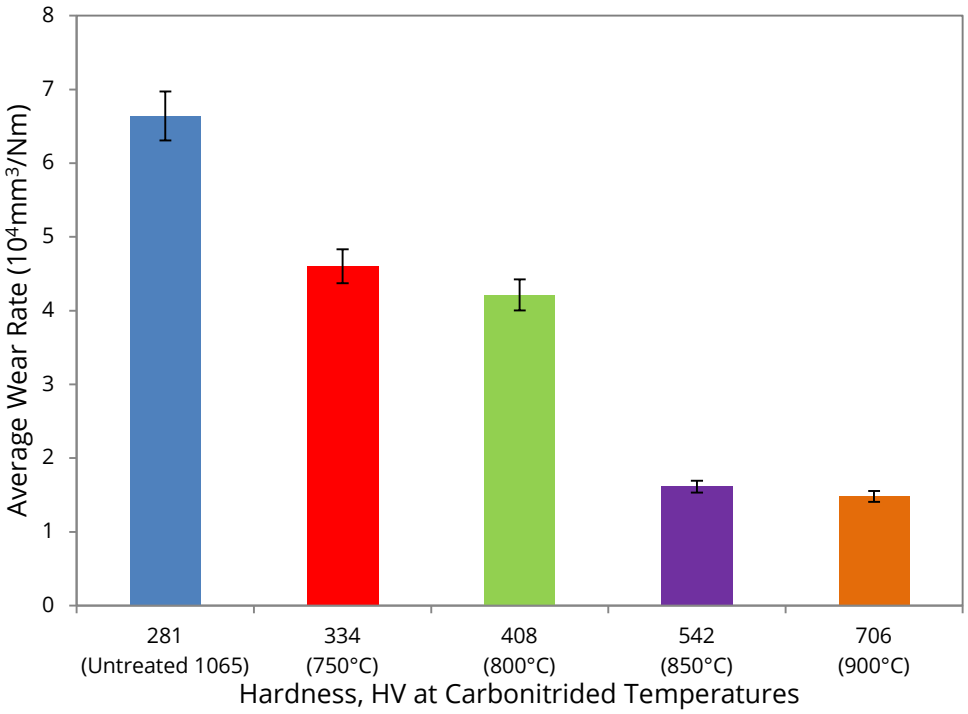

Figure 4-16: Total Weight Losses Against Varying Hardness of AISI 1065 Steel that was Carbonitrided at Different Temperatures for 5hrs, Water-Quenched and Tempered at 300C for 3hrs.

5.0 Conclusions, Recommendations and Future Work

5.1 Conclusions

1. At 900℃, carbonitrided (5hrs), quenched and tempered (300℃, 3hrs) 1065 steel gave:
    - Highest surface hardness of **706 HV** from **281 HV.**
    - Improved strength from **948** to **978 MPa**.
    - Lowest coefficient of friction.
    - Lowest wear rate.
2. Hardening steel with pulverized cassava leaves is **cost-effective** (waste to wealth)**, safe** and **has wide applications.**
3. The economic implication of result shows that **machine downtime** and **cost of replacing mining tools** can be reduced**.**

5.2 Recommendations

The following are recommendations for future work:

1. Carbonitriding at lower temperatures in order to favor the diffusion of nitrogen against carbon at lower temperatures.
2. Analytical and computational modelling of diffusion kinetics.
3. Determination of stress intensity and fracture toughness of the steel.

5.3 Future Works

The geometries of the pickax, power shovel and jaw crusher were modelled as shown in Figs 5.1 to 5.3. Their respective mechanical properties are detailed in Tables 5.1 to 5.5. Analyses are to be conducted to achieve the following:

- Verify the stress distributions on these tools under industry loading conditions.
- Improve the impact/performance of these tools with respect to small-scale and large-scale applications, without (significant) increase in weight.
- Compare stress distribution of carbonitrided 1065 (quenched and tempered) steel with industry manganese steel properties.

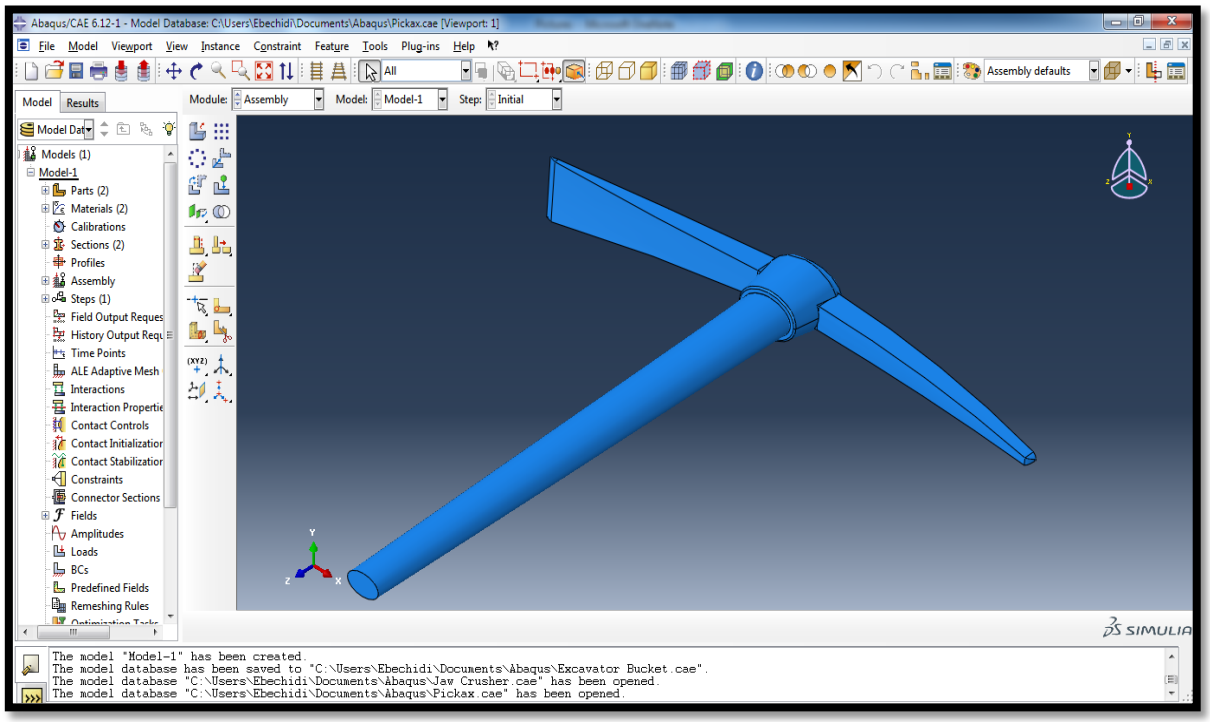

Figure 5-1: Pickax geometry in CAE AbaqusTM 6.12 software.

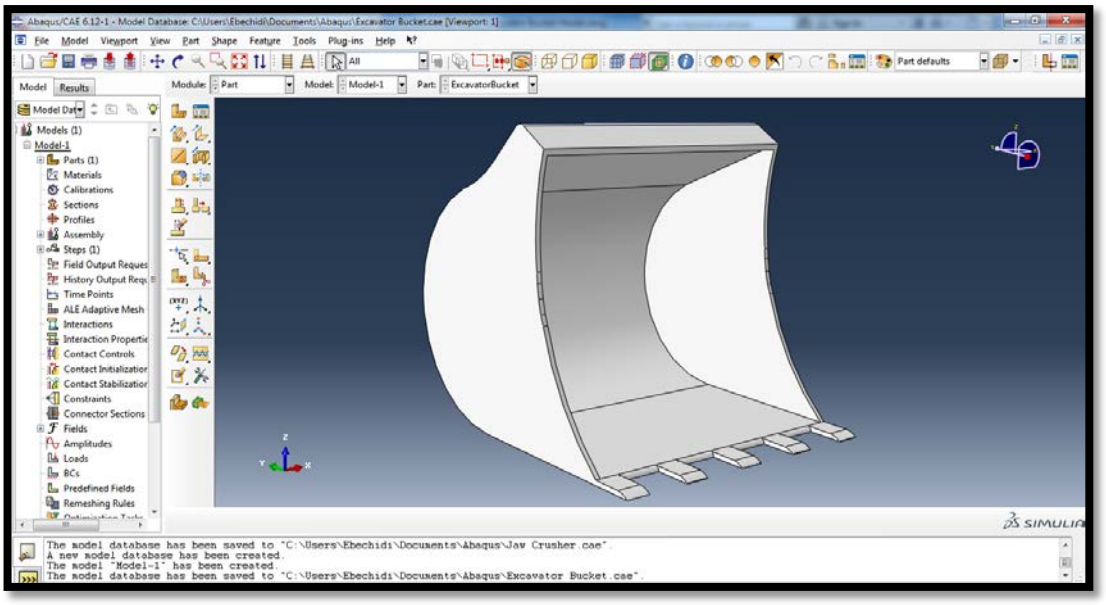

Figure 5-2: Excavator bucket geometry in CAE AbaqusTM 6.12 software.

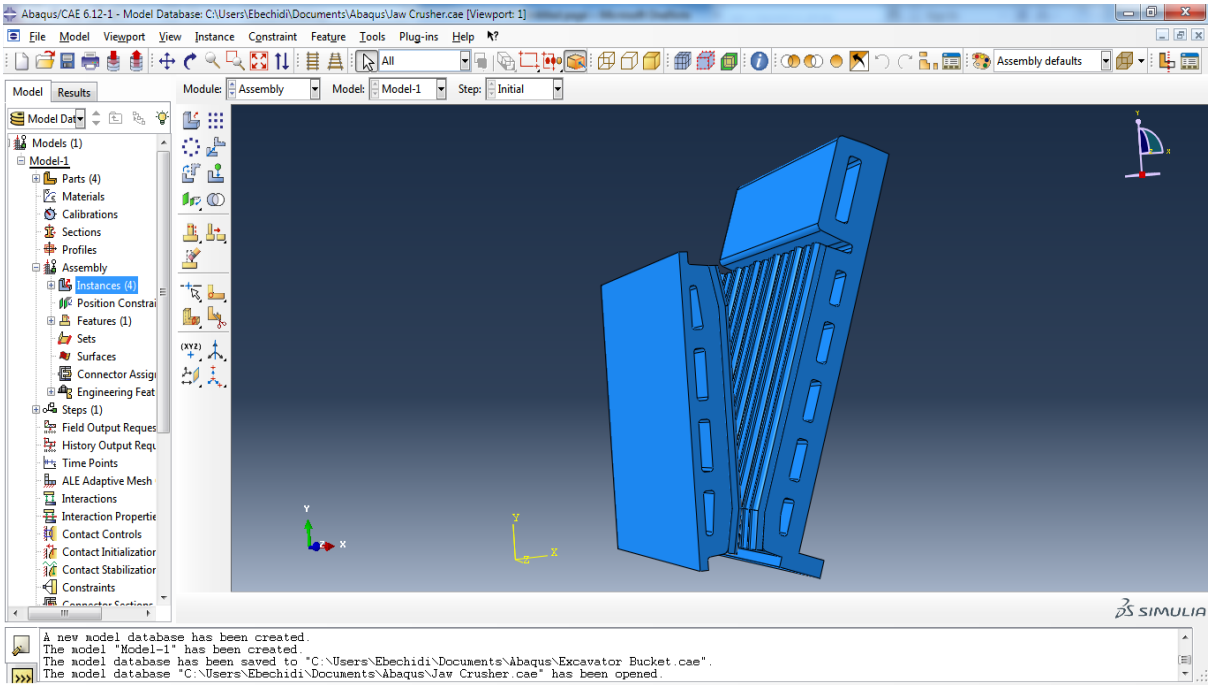

Figure 5-3: A section of Jaw crusher geometry in CAE AbaqusTM 6.12 software.

Table 5-1: Barite mechanical properties for modeling.

Bulk modulus, B	**49.5 GPa**
Shear modulus, G	**19.81 GPa**
Young's modulus, E	**52.43 GPa**
Poisson ratio, υ	**0.32**

Table 5-2: Wood mechanical properties for modeling.

Young's modulus, E (Teak - assumed)	**12.5 GPa**
Poisson ratio, υ	**0.38**

Table 5-3: Mechanical properties of 1065 steel for modeling.

*Young's modulus, E	**210 GPa**
Yield strength, σ_y (Computed)	**948 GPa**
*Poisson ratio, υ	**0.29**
Assumed body force	**100 N**
Linear Extension, LE	**0.6 mm**
Density, ρ	**7.8g/cm^3** = **7800kg/m^3**

**Ashbey, CES Edupack 2011*[41].

Table 5-4: Mechanical properties of carbonitrided 1065 steel for modeling.

Assumed Young's modulus, E	**200 GPa**
Yield strength, σ_y (Computed)	**978 GPa**
*Poisson ratio, υ	**0.29**
Assumed body force	**100 N**
Linear Extension, LE	**0.45 mm**
Density, ρ	**7.87g/cm^3 = 7870kg/m^3**

**Ashbey, CES Edupack 2011*[41].

Table 5-5: CAT 6030/6030 FS excavator bucket data for modeling*.

Operating weight	**294 tonnes (324 tons)**
Engine output	**1140 kW (1,530 hp)**

* *Adapted from CAT website.*

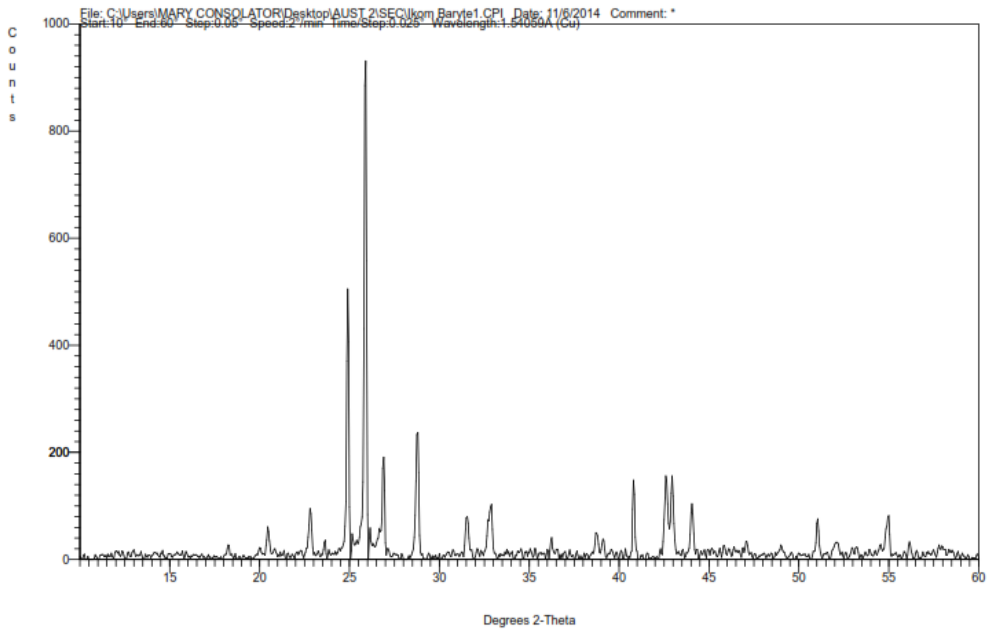

Figure 5-4: XRD analysis of barite from Ikom, Cross Rivers – Nigeria, characterized at Engineering Materials Development Institute, EMDI - Akure, Nigeria.

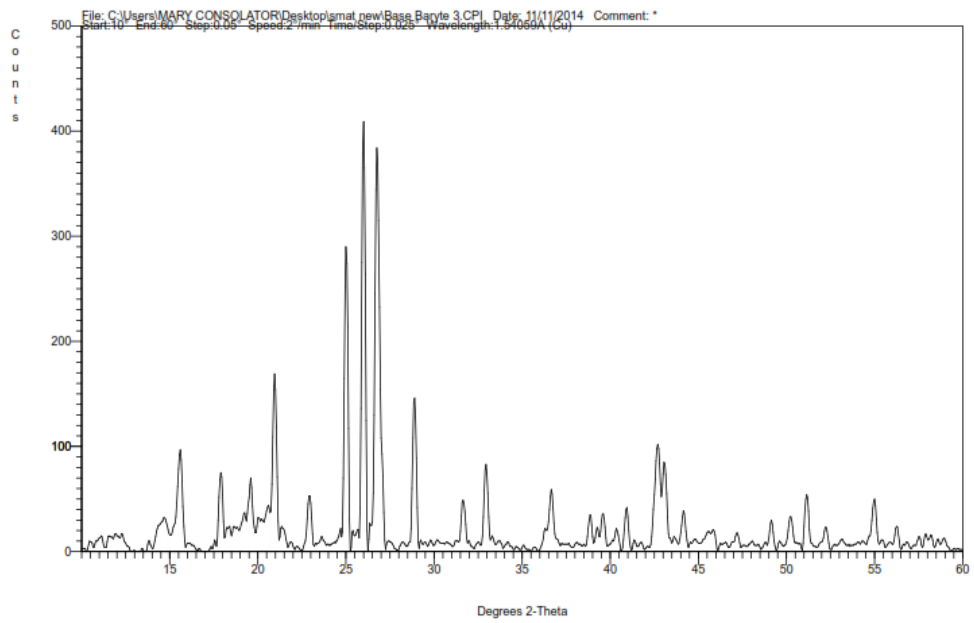

Figure 5-5: XRD analysis of barite from Biase, Cross Rivers – Nigeria, characterized at Engineering Materials Development Institute, EMDI - Akure, Nigeria.

The chart below (Fig. 5.6) relates moh's hardness of minerals to their Vickers hardness values. This is to help compute the relative hardness of all the constituent minerals in a deposit. Note that the chart is not adaptable for metals.

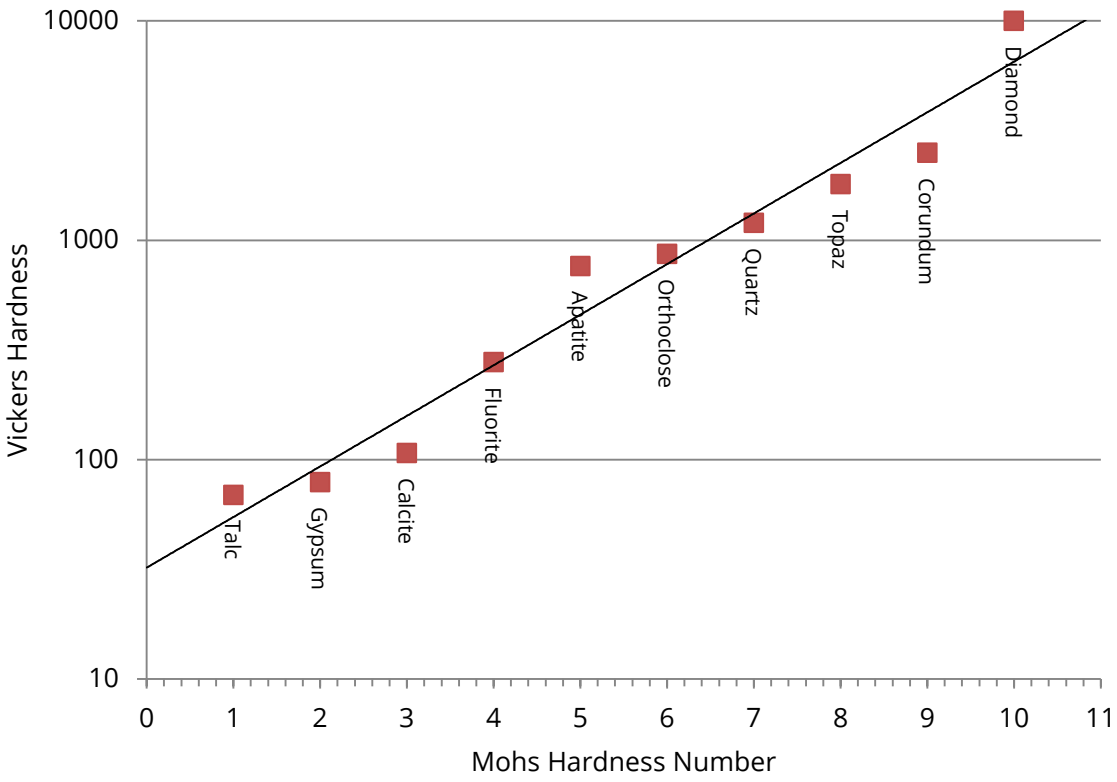

Figure 5-6: Relation Between Vickers & Mohs Hardness[43].

The understanding gained from these studies would help the development of simple mechanized power shovel equipment for mining and construction purposes. The equipment does not have to be of similar size and capacity of regular excavators or pay-loaders. Once the device can be fixed and mounted on the floor, and can exert required force, fork lift and dump away excavated product, it would certainly be a major improvement from the regular hand-digger, hand-shovel and hoe.

References

[1] M. M. Miller, *Minerals Yearbook*. 2009.

[2] "No Title," *Exploring the North*. [Online]. Available: www.exploringthenorth.com/cophistory/cophist.html. [Accessed: 23-Sep-2014].

[3] S. Evans, "Lubrication Management Systems," *A Noria Publication*, 2002. [Online]. Available: www.machinerylubrication.com/Read/3. [Accessed: 23-Sep-2014].

[4] J. Williams, "Wear and surface damage," in *Engineering Tribology*, 1st ed., Cambridge University Press, 2005, pp. 166–199.

[5] J. D. Bressan, D. P. Daros, A. Sokolowski, R. A. Mesquita, and C. A. Barbosa, "Influence of hardness on the wear resistance of 17-4 PH stainless steel evaluated by the pin-on-disc testing," *J. Mater. Process. Technol.*, vol. 5, no. 205, pp. 353–359, 2007.

[6] J. D. Bressan and R. Hesse, "Construction and validation tests of a pin-on-disc equipment.," *Congr. Bras. Eng. Mec.*, vol. 16, 2001.

[7] MMSD, "Barites From MMSM.pdf," Abuja.

[8] M. S. Chaanda, N. G. Obaje, A. Moumouni, N. G. Goki, and U. A. Lar, "Environmental Impact of Artesanal Mining of Barytes in Azara Area, Middle Benue Trough, Nigeria," *Medwell Journals*, vol. 4, no. 1, pp. 38 – 42, 2010.

[9] A. C. Achusim-Udenko, O. Gerald, O. Martins, and A. Ausaji, "FLOTATION RECOVERY OF BARITE FROM ORE USING PALM BUNCH BASED COLLECTOR," *Int. J. Chem. Sci.*, vol. 9, no. 3, pp. 1518–1524.

[10] "Barite Mining." [Online]. Available: http://www.shibang-china.com/application/barite-mining.html. [Accessed: 25-Aug-2014].

[11] W. F. Smith, "Surface Hardening and Surface Modification of Metals," in *Structure and Properties of Engineering Alloys*, Second., Orlando, Florida: McGraw-Hill, 1993, pp. 591–613.

[12] C. Li, Q. He, W. Tang, and F. Lu, "N," *Surf. Coat. Technol.*, vol. 187, p. 1, 2004.

[13] J. M. Baek, Y. R. Cho, D. J. Kim, and K. H. Lee, "No Title," *Surf. Coat. Technol.*, vol. 131, p. 568, 2000.

[14] B. Edenhofer, W. Grafen, and J. M. Zller, "No Title," *Surf. Coat. Technol.*, vol. 142–144, p. 225, 2001.

[15] H. Jime'nez, M. H. Staia, and E. S. Puchi, "No Title," *Surf. Coat. Technol.*, vol. 120–121, p. 358, 1999.

[16] S. Azuar, A. Azis, I. Jauhari, and N. W. Ahamad, "Surface & Coatings Technology Improving surface properties and wear behaviors of duplex stainless steel via pressure carburizing," *Surf. Coat. Technol.*, vol. 210, no. 2012, pp. 142–150.

[17] B. Selcuk, R. Ipek, and M. B. Karamıs, "A study on friction and wear behaviour of carburized , carbonitrided and borided AISI 1020 and 5115 steels," vol. 141, no. 2003, pp. 189–196, 2002.

[18] O. J. Ibironke, A. Falaiye, T. V. Ojumu, E. A. Odo, and O. O. Adewoye, "Case depth studies of pack cyaniding of mild steel using cassava leaves," *Mater. Manuf. Process.*, vol. 19, no. 5, pp. 899–905, 2004.

[19] S. R. A. Adewusi, T. V. Ojumu, and O. S. Falade, "The effect of processing on total organic acids contents and mineral availability of stimulated cassava-vegetable diets.," *Plants Food Hum. Nutr.*, vol. 53, pp. 367–380, 1999.

[20] D. A. (The G.-W. C. I. . I. Brandt, "No Title," *Metall. Fundam.*, pp. 223–243, 1985.

[21] G. Celebi, M. Ipek, C. Bindal, and A. H. Ucisik, "Some mechanical properties of borides formes on AISI 8620 steel," *Mater. Forum*, vol. 29, pp. 456–460, 2009.

[22] M. Tabur, M. Izciler, F. Gul, and I. Karacan, "Abrasive wear behavior of boronized AISI 8620 steel," vol. 266, no. 2009, pp. 1106–1112, 2000.

[23] C. Martini, G. Palombarini, G. Poli, and D. Prandstraller, "Sliding and abrasive wear behaviour of boride coatings," *Wear*, vol. 256, pp. 608–614, 2004.

[24] K. H. Habig and R. Chatterjee-Fischert, "Wear behaviour of boride layers alloyed steels," *Tribol. Int.*, vol. August, pp. 209–215, 1981.

[25] B. Venkataraman and G. Sundararajan, "The high speed sliding wear behaviour of boronied medium carbon steel," *Surf. Coat. Technol.*, vol. 73, pp. 177–184, 1995.

[26] A. K. Sinha, "ASM Handbook," *ASM Int.*, vol. 4, p. 437, 1991.

[27] T. S. Eyre, "Effect of boronising on friction and wear of ferrous metals," *Wear*, vol. 34, pp. 383–397, 1975.

[28] V. Jain and G. Sundararajan, "Influence of the pack thickness of the boronizing mixture on the boriding of steel," *Surf. Coat. Technol.*, vol. 149, pp. 21–26, 2002.

[29] O. Ozdemir, M. Usta, C. Bindal, and A. H. Ucisik, "Hard iron boride (Fe2B) on 99.97 wt% pure iron," *Vacuum*, vol. 80, pp. 1391 – 1395, 2006.

[30] C. Meric, S. Sahin, B. Backir, and N. S. Koksal, “Investigation of the boronizing effect on the abrasive wear behavior in cast irons,” *Elsevier*, vol. 27, pp. 751 – 757, 2006.

[31] W. D. Callister(Jr.) and D. G. Rethwisch, *Material Science and Engineering: An Introduction*, 8th ed. Utah and Iowa: John Wiley and Sons, 2010, pp. 281–290.

[32] R. G. Bayer, *Mechanical Wear Fundametals and Testing*, 2nd ed. New York: Marcel Dekker Inc., 2004.

[33] W. Conshohocken, “Standard Test Method for Wear Testing with a Pin-on-Disk Apparatus,” United States, 2000.

[34] J. F. Molinari, M. Ortiz, R. Radovitzky, and E. A. Repetto, “Finite-element modeling of dry sliding wear in metals,” *CALTECH ASCI Tech. Rep. 079*, vol. 18, no. 3/4, pp. 592–609, 2001.

[35] M. Izciler and H. Celik, “Two and three body wear behaviour of different heat treated boron alloyed high chromium cast iron grinding balls,” *J. Mater. Process. Technol.*, vol. 105, p. 237, 2000.

[36] M. Izciler and M. Muratoglu, “Wear behaviour of SiC reinforced 2124 Al alloy composite in RWAT system,” *J. Mater. Process. Technol.*, vol. 132, p. 67, 2003.

[37] M. Izciler and M. Tabur, “Abrasive wear behaviour of different case depth gas carburized AISI 8620 gear steel,” *Wear*, vol. 260, pp. 90–98, 2006.

[38] W. F. Smith, *Structure and Properties of Engineering Alloys*, 2nd ed. Florida: McGraw-Hill, 1993, pp. 82–175,591–613.

[39] C. L. Briant and S. K. Banerji, “No Title,” *Int. Met. Rev.*, vol. 23, no. 4, p. 232, 1978.

[40] W. M. Imrie, “No Title,” *Roy. Soc. Lond. Phil. Trans.*, vol. A, no. 282, p. 91, 1976.

[41] M. Ashby, “CES EduPack 2011.” p. AISI 1060, Oil–quenched & Tempered @ 300°C, 2011.

[42] S. C. Lim and M. F. Ashby, “Wear mechanism maps,” *Acta Metall.*, vol. 35, no. 1, pp. 1–24, 1987.

[43] W. F. Hosford, *Mechanical Behavior of Materials*. USA: Cambridge University Press, 2005, p. 66.

[44] U. Ulusoy and M. Yekeler, “Floatability of barite particles with different shape and roughness,” *Indian J. Chem. Technol.*, vol. 14, no. November, pp. 616–625, 2007.

Appendix

A. Chemical Analysis Results

CERTIFICATE OF ANALYSIS

N°: Date: 22/10/14

Ref. Alloy: Operator: YUSUF

Customer: AFRICAN UNIVERSITY

Order:

This is to certify that the goods

Goods:

Sample: SAMPLE A
Cast:
Qt:

have this chemical analysis:

	C%	Si%	Mn%	P%	S%	Cr%	Mo%	Ni%	Nb%
Report	0.616	0.188	0.724	0.029	0.015	0.048	<0.002	0.032	<0.002
Ref. MIN	-----	-----	-----	-----	-----	-----	-----	-----	-----
Ref. MAX	-----	-----	-----	-----	-----	-----	-----	-----	-----

	Al%	Cu%	Co%	B%	Ti%	V%	W%	Mg%	Ca%
Report	<0.001	0.036	0.006	<0.0005	0.009	<0.001	0.007	0.0014	0.0059
Ref. MIN	-----	-----	-----	-----	-----	-----	-----	-----	-----
Ref. MAX	-----	-----	-----	-----	-----	-----	-----	-----	-----

	Ce%	La%	As%	Pb%	Sn%	Sb%	Te%	Zn%	Zr%
Report	<0.002	0.005	0.006	<0.002	<0.001	<0.005	<0.001	<0.001	<0.001
Ref. MIN	-----	-----	-----	-----	-----	-----	-----	-----	-----
Ref. MAX	-----	-----	-----	-----	-----	-----	-----	-----	-----

	N%	Fe%							
Report	0.044	98.222							
Ref. MIN	-----	-----							
Ref. MAX	-----	-----							

Notes :

Fig A1: Chemical analysis of sample A, representing the NEW PICKAX, analyzed at SCC Pipe Yard, Bwari, Abuja – Nigeria.

CERTIFICATE OF ANALYSIS

N°: Date: 22/10/14

Ref. Alloy: Operator: YUSUF

Customer: AFRICAN UNIVERSITY

Order:

This is to certify that the goods

Goods:

Sample: SAMPLE B
Cast:
Qt:

have this chemical analysis:

	C%	Si%	Mn%	P%	S%	Cr%	Mo%	Ni%	Nb%
Report	0.749	0.142	0.968	0.024	0.006	0.019	<0.002	<0.002	<0.002
Ref. MIN	-----	-----	-----	-----	-----	-----	-----	-----	-----
Ref. MAX	-----	-----	-----	-----	-----	-----	-----	-----	-----

	Al%	Cu%	Co%	B%	Ti%	V%	W%	Mg%	Ca%
Report	0.002	0.005	0.002	<0.0005	0.011	<0.001	0.008	0.0014	0.0059
Ref. MIN	-----	-----	-----	-----	-----	-----	-----	-----	-----
Ref. MAX	-----	-----	-----	-----	-----	-----	-----	-----	-----

	Ce%	La%	As%	Pb%	Sn%	Sb%	Te%	Zn%	Zr%
Report	<0.002	<0.005	<0.005	0.002	<0.001	<0.005	<0.001	<0.001	<0.001
Ref. MIN	-----	-----	-----	-----	-----	-----	-----	-----	-----
Ref. MAX	-----	-----	-----	-----	-----	-----	-----	-----	-----

	N%	Fe%							
Report	0.033	98.014							
Ref. MIN	-----	-----							
Ref. MAX	-----	-----							

Notes :

Fig A2: Chemical analysis of sample B, representing the OLD PICKAX, analyzed at SCC Pipe Yard, Bwari, Abuja – Nigeria.

B. SEM Image of Fractured Surfaces

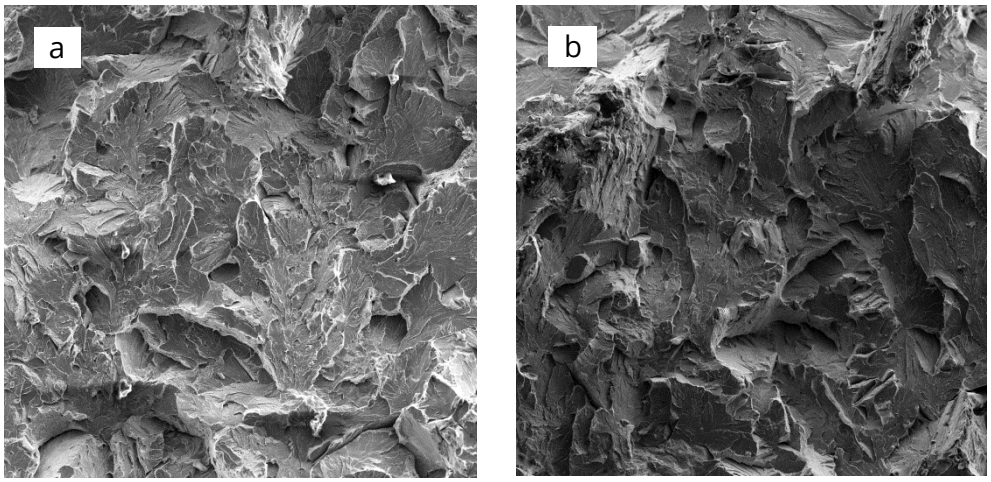

Fig B1: Microstructure of the fractured surface at 250 magnification using SEM for a) 1065 steel, b) 1070 steel.

C. Lim & Ashby Chart Formulae:

Normalized Pressure, ~P: $\frac{P}{H},\ P\ - Pressure \frac{Load}{A_{nom}},\ H - Hardness$

Normalized Velocity, Ũ: $\frac{U}{k}\sqrt{\frac{A_{nom}}{\pi}},\ U\ - Velocity,\ k - Thermal\ Diffusivity$

Thermal Diffusivity, k: $\frac{Thermal\ Conductivity}{Density\ x\ Specific\ Heat}$

Wear Rate, w̃: $\frac{w}{A_{nom}},\ w\ - wear\ rate, A_{nom} - Nominal\ Area$

(Lim and Ashby, 1987)